MATHEMATICAL BIOSCIENCES
AND ENGINEERING
Volume **10**, Number **4**, August **2013**

doi:10.3934/mbe.2013.10.1095

pp. **1095–1133**

REGULATION OF TH1/TH2 CELLS IN ASTHMA DEVELOPMENT: A MATHEMATICAL MODEL

Yangjin Kim†

Department of Mathematics
Konkuk University
Seoul, Republic of Korea

Seongwon Lee

Department of Mathematics
Pohang University of Science and Technology
Pohang, Gyeongbuk, Republic of Korea

You-Sun Kim

Department of Life Science
Pohang University of Science and Technology
Pohang, Gyeongbuk, Republic of Korea

Sean Lawler

Leeds Institute of Molecular Medicine
University of Leeds
Leeds, United Kingdom

Yong Song Gho and Yoon-Keun Kim

Department of Life Science
Pohang University of Science and Technology
Pohang, Gyeongbuk, Republic of Korea

Hyung Ju Hwang‡

Department of Mathematics
Pohang University of Science and Technology
Pohang, Gyeongbuk, Republic of Korea

(Communicated by Heiko Enderling)

2010 *Mathematics Subject Classification.* Primary: 92C45, 92C50; Secondary: 92B05.

Key words and phrases. Asthma, Th1/Th2 cells, microenvironment, LPS, inflammation.

†Y. Kim is supported by the National Science Foundation upon agreement 112050 and DMS-1135663, the Rackham Grant at University of Michigan-Ann Arbor, Faculty Research Grant at University of Michigan-Dearborn, and the Basic Science Research Program through the National Research Foundation of Korea by the Ministry of Education and Technology (2012R1A1A1043340).

‡H.J. Hwang is supported by the Basic Science Research Program through the National Research Foundation of Korea funded by the Ministry of Education, Science and Technology (2010-0008127).

Abstract. Airway exposure levels of lipopolysaccharide (LPS) determine type I versus type II helper T cell induced experimental asthma. While high LPS levels induce Th1-dominant responses, low LPS levels derive Th2 cell induced asthma. The present paper develops a mathematical model of asthma development which focuses on the relative balance of Th1 and Th2 cell induced asthma. In the present work we represent the complex network of interactions between cells and molecules by a mathematical model. The model describes the behaviors of cells (Th0, Th1, Th2 and macrophages) and regulatory molecules (IFN-γ, IL-4, IL-12, TNF-α) in response to high, intermediate, and low levels of LPS. The simulations show how variations in the levels of injected LPS affect the development of Th1 or Th2 cell responses through differential cytokine induction. The model also predicts the coexistence of these two types of response under certain biochemical and biomechanical conditions in the microenvironment.

1. **Introduction.** Asthma is a common chronic inflammatory disorder of the airways associated with reversible airway obstruction and airway hyperresponsiveness (AHR) [25, 13]. There are approximately 300 million asthmatics worldwide [69, 64]. The symptoms of asthma include wheezing, coughing, chest tightness and shortness of breath. To avoid unnecessary inflammatory responses, the immune response to inhaled inert antigens (allergens) involves non-responsive processes such as tolerance and ignorance [35, 2]. The development of memory T cells to inhaled allergens is a critical event in initiation and orchestration of the inflammatory response in asthmatic airways [104, 39]. Lipopolysaccharide (LPS) that is a cell wall component of gram-negative bacteria, present in the air including dust particles [71, 35]. LPS is a pathogen-associated molecular pattern (PAMP) that is recognised by its receptor TLR4, and induced pro-inflammatory and immune-modulated mediators such as IL-12 and TNF-α [60, 29]. In previous studies, inhalation of various doses of LPS-contaminated inert allergen caused the breakdown of immune tolerance and induction of an allergen immune response in the airway [53]. See Figure 1. The immune responses to inhaled antigens are mainly dependent on antigen-specific helper T cells (Th cells). Antigens presented by dendritic cells and B cells interact with TCR (T cell receptors) on antigen inexperienced naive T cells which then proliferate and differentiate into antigen specific T cells known as memory T cells. Differentiated memory T cells divide into three subtypes, Th1, Th2, and Th17 that were recently discovered to constitute a separate subset [77, 102, 62]. Naive T cells stimulated by IL-12 transduce intracellular signals including a transcription factor, T-bet, and differentiate into IFN-γ producing Th1 cells [66]. Th2 cells develop in response IL-4 and a transcription factor, GATA3, and produce IL-4, IL-5, and IL-13. The immune response mediated by Th1 and Th2 cells induces non-eosinophilic (neutrophilic) inflammation and eosinophilic inflammation, respectively [7, 53] (see Figure 2). Ruedl *et al.* (2000) [91] found that high doses of antigen induced the Th1 responses while the low lose antigen stimulation led to the Th2 responses. On the other hand, Eisenbarth *et al.* [29] found that high (100 μg) and low (0.1 μg) levels of inhaled LPS in a mouse model of allergic sensitization induced Th1 and Th2 responses, respectively. Using an Ovalbumin (OVA) model, commonly used to stimulate an allergic reaction in test subjects, Kim *et al.* (2007) [53] investigated the effect of airway exposure of LPS on Th1/Th2 regulation of allergy development using mouse and human data. This study further suggested that airway exposure levels of high and low LPS can lead to type I and type II asthma phenotypes,

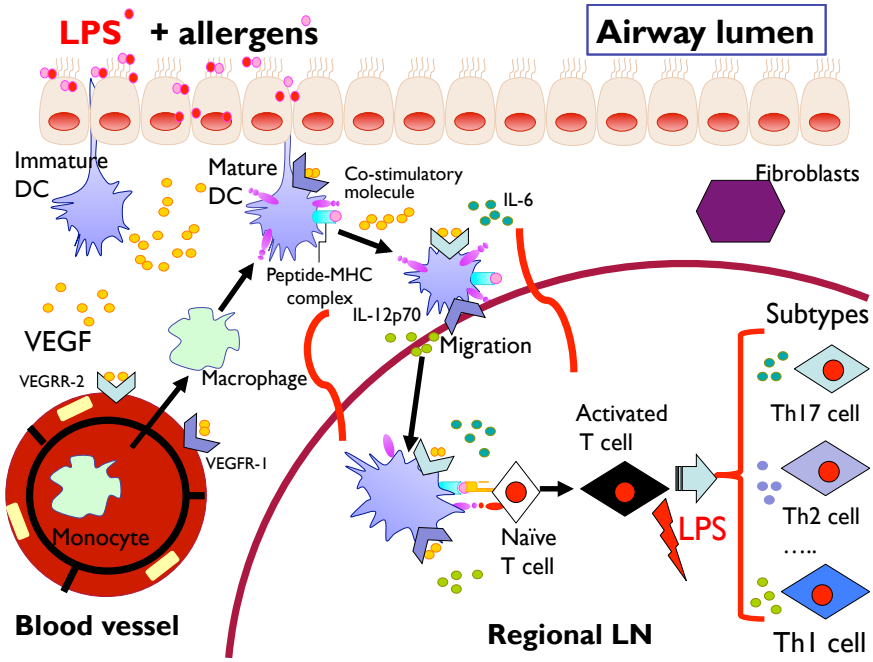

FIGURE 1. Schematics of asthma development (based on [53, 73, 77, 102, 62, 41, 6, 23]). VEGF = Vascular Endothelial Growth Factor, DC = Dendritic Cells, LN = Lymph Node.

respectively. These experiments [29, 53] suggest that the airway allergen sensitization by LPS induces asthma that is differentially regulated according to LPS levels. See Figure 2. The immune system consists of a complex network of cells and molecules that communicate with each other via nonlinear interactions, and these nontrivial intracellular behaviors have been analyzed through mathematical models [19]. These include Fas-mediated activation-induced cell death in Th1/2 regulation [109] and detailed regulation of T-bet and GATA3 in Th1 and Th2 differentiation [110]. Other authors investigated Th1-Th2 regulation with various approaches [74, 30, 31, 32, 20, 79, 10, 11, 88, 101, 38] (Some discussions on these models can be found in [109]). In this paper we develop a more comprehensive model of Th1/2 regulation in asthma development via LPS regulation.

Our goal in this paper is to present a mathematical model that is able to explain this Th1-Th2 regulation via the complex crosstalk between various cells and cytokines. The model was described by a system of partial differential equations (PDEs) of densities of key cells (Th1 cells, Th2 cells, Th0 cells, and macrophages) and concentrations of central regulating factors (IFN-γ, IL-4, IL-12, and TNF-α).

In Section 2, we introduce and describe a mathematical model. In Section 3 we present the simulation results. In Section 4, we discuss our results and future work. Parameter estimation and nondimensionalization are provided in Appendix A and B respectively. Sensitivity analysis of the model system was performed in Appendix C.

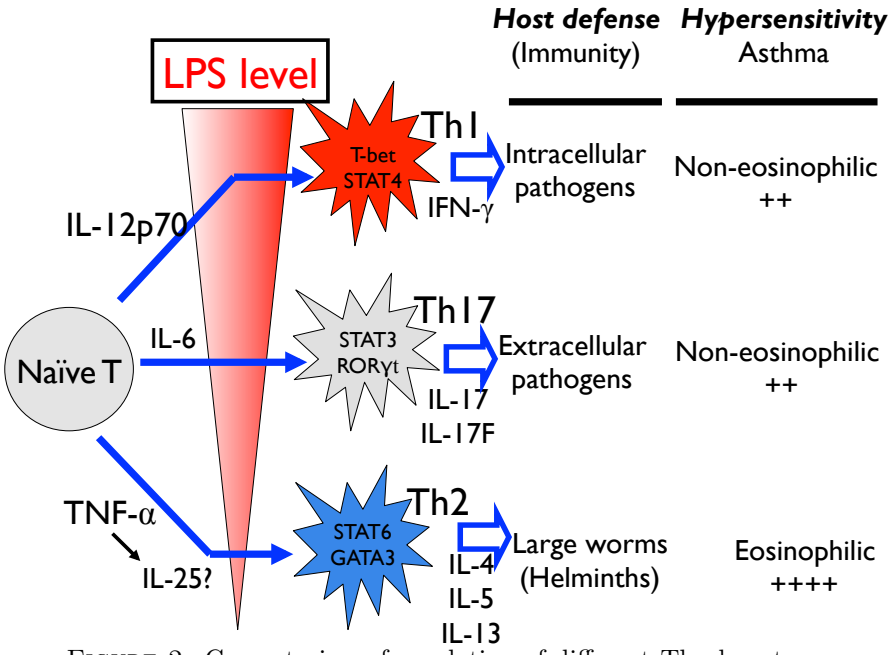

FIGURE 2. Current view of regulation of different Th phenotypes (Th1 and Th2, and Th17) in asthma development. High levels of LPS lead to Th1 cell induced asthma and low doses of LPS induce Th2 cell induced asthma. Intermediate (or relatively high) levels of LPS can generate the Th17 phenotype in a perturbed system via IL-6 and IL-17 [53, 73, 77, 102, 62, 41].

2. **Mathematical model.** In this section, we derive the governing equations of densities of Th1 cells, Th2 cells, Th0 cells and macrophages, and concentrations of IFN-γ, IL-4, IL-12, and TNF-α using a system of PDEs.

2.1. **Th1 cell density ($=H_1(x,t)$).** The mass balance equation for Th1 cell density is

$$\frac{\partial H_1}{\partial t} + \nabla \cdot J = P_n, \tag{1}$$

where J is the flux of the cells and P_n is the production/death of cells. Only contribution of the flux J is from random motility of the cells, *i.e.,* Th1 cells move in random motion,

$$J = J_{\text{random}} = -D_{H_1} \nabla H_1, \tag{2}$$

where D_{H_1} is the random motility constant.

It has been shown that Th1 cells are produced when dendritic cells and pre-Th cells form an immunological synapse in which the dendritic cell presents antigen to the T cell's receptor for antigen, and secretes several factors including interleukin 12 (IL-12). It is also known that an addition of IL-12 increases Th1 differentiation [98] and IL-12 secreted from macrophages assists this process. However, IL-4 inhibits the production of Th1 cells from Th0 cells. See Figure 3. We assume that Th1 cells are differentiated from Th0 cells with the carrying capacity K_1. We also take

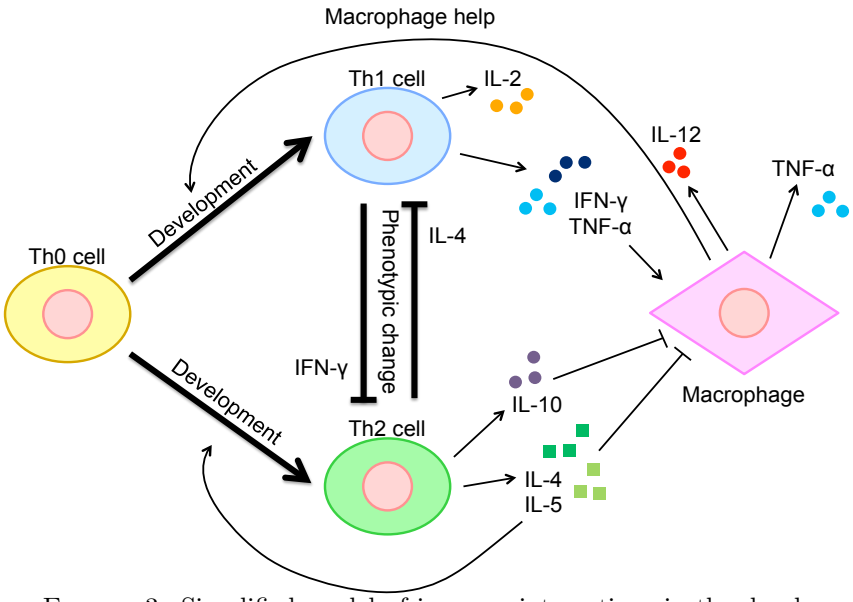

FIGURE 3. Simplified model of immune interactions in the development of asthma. The model shows the cytokines secreted by key cell types, Th1 and Th2 cells, and how they regulate each other. Arrows means secretion or activation. For example, Th1 cells secrete IFN-γ. Hammerheads mean inhibition. Details of the mechanism are discussed in [42] and others.

into consideration *apoptosis* (programmed cell death) with the cell death rate μ_{H_1}. Taking into account these observations, the production/death term is given by

$$P_n = \frac{\lambda_5 I_2}{\lambda_6^m + I_1^m} H_0 H_1 \left(1 - \frac{H_1}{K_1}\right) - \mu_{H_1} H_1, \tag{3}$$

where $I_1 (= I_1(x,t))$ is the concentration of IL-4 described in Section 2.6 below, $I_2 (= I_2(x,t))$ is the concentration of IL-12 described in Section 2.7 below, $H_0 (= H_0(x,t))$ is the density of Th0 cells in Section 2.3 below, λ_5 is the IL-12 mediated proliferation rate of Th1 cells, m is the Hill-type function exponent with the inhibition parameter λ_6 of Th1 cell proliferation by IL-4.

In summary, we have the following governing equation for the Th1 cell density:

$$\frac{\partial H_1}{\partial t} = \underbrace{D_{H_1} \Delta H_1}_{\text{Random motility}} + \underbrace{\frac{\lambda_5 I_2}{\lambda_6^m + I_1^m} H_0 H_1 \left(1 - \frac{H_1}{K_1}\right)}_{\text{proliferation}} - \underbrace{\mu_{H_1} H_1}_{\text{death}}. \tag{4}$$

2.2. **Th2 cell density ($=H_2(x,t)$).** As in the case of Th1 cell density, the same form of the mass balance equation applies to Th2 cell density with the flux J due to random motility

$$J = J_{\text{random}} = -D_{H_2} \nabla H_2, \tag{5}$$

where D_{H_2} is the random motility of Th2 cells.

The production of Th2 cells is mediated by IL-4 but can be inhibited by IFN-γ (the second term in equation (6) below). In a previous study [48], it has been

observed that the allergen sensitization with low-dose LPS was associated with up-regulation of TNF-α production during allergen sensitization. This may be contradictory to the classical finding that TNF-α is secreted by Th1 cells and recruits macrophages, which, in turn, promotes Th1 development [42]. More importantly, it is LPS-dependent. We assume that the proliferative potential of Th2 cells is increased in the presence of TNF-α and abundant IL-4 but decreased in the presence of IFN-γ based on the findings in [48] and others. (See Figure 3.) This leads to the following governing equation for the Th2 cell density

$$\frac{\partial H_2}{\partial t} = \underbrace{D_{H_2}\Delta H_2}_{\text{Random motility}} + \underbrace{\frac{\lambda_2 T I_1}{\lambda_7^k + F^k} H_0 H_2 \left(1 - \frac{H_2}{K_2}\right)}_{\text{proliferation}} - \underbrace{\mu_{H_2} H_2}_{\text{death}}, \tag{6}$$

where λ_2 is the proliferation rate of Th2 cells, $T(= T(x,t))$ is the concentration of TNF-α described in Section 2.8 below, λ_7 is the inhibition parameter of Th2 cell proliferation by IFN-γ with the Hill function exponent k, $F(= F(x,t))$ is the IFN-γ concentration described in Section 2.5 below, K_2 is the carrying capacity of Th2 cells, and μ_{H2} is the death rate of Th2 cells.

2.3. **Th0 cell density ($=H_0(x,t)$).** As in the cases of Th1 and Th2 cells, the only contribution for the flux would be the flux due to random motility of Th0 cells: $J = J_{\text{random}} = -D_{H_0}\nabla H_0$ where D_{H_0} is the random motility constant of Th0 cells. With a source of β, these Th0 cells are developed to Th1 and Th2 phenotypes (Figure 3) and they also undergo apoptosis with the death rate μ_{H0}. Therefore, this Th0 population serves as a source for Th1 and Th2 populations in the model. The governing equation for this naive cell density (H_0) is then described by

$$\frac{\partial H_0}{\partial t} = \underbrace{D_{H_0}\Delta H_0}_{\text{Random motility}} + \underbrace{\beta}_{\text{input}} - \left(\underbrace{\frac{\lambda_5 I_2}{\lambda_6^m + I_1^m} H_0 H_1}_{\text{Th0}\to\text{Th1}} + \underbrace{\frac{\lambda_2 T I_1}{\lambda_7^k + F^k} H_0 H_2}_{\text{Th0}\to\text{Th2}} \right) - \underbrace{\mu_{H_0} H_0}_{\text{death}}, \tag{7}$$

where the third and fourth terms describe the loss of the Th0 cell population due to their conversions to Th1 (H_1) and Th2 (H_2) subtypes.

2.4. **Macrophage density ($=M(x,t)$).** The mass balance equation for the macrophage density is

$$\frac{\partial M}{\partial t} + \nabla \cdot J = P_M \tag{8}$$

where J is the flux of the cells and P_M is the production/death of cells. The flux J is split into two different parts,

$$J = J_{\text{random}} + J_{\text{chemo}} \tag{9}$$

where J_{random} is the flux due to random motion and J_{chemo} is the flux due to *chemotaxis*, that is, cell migration toward a certain high chemical gradient. The flux due to random motion is calculated in a similar fashion,

$$J_{\text{random}} = -D_M \nabla M, \tag{10}$$

where D_M is the random motility constant of macrophages. In the case of macrophages, it is known that macrophages are co-localized with Th1 cells and it is assumed

that macrophages migrate toward Th1 cells using IFN-γ as a chemokine. In other words, macrophages are attracted to the gradient of IFN-γ (*chemotaxis*). This is often written in the form $M\bar{\chi}(\nabla F)$ where $\bar{\chi}$ is a constant. We assume that the chemotactic attraction remains bounded even as ∇F becomes very large, and use the following form of chemotactic attraction from [51], $\chi\frac{M\nabla F}{\sqrt{1+\lambda_F|\nabla F|^2}}$, where λ_F is a positive constant and χ is the chemotactic coefficient. As noted in [51], λ_F is set to be zero ($\lambda_F = 0$) in most articles. Then, the chemotactic flux is described by

$$J_{\text{chemo}} = \chi\frac{M\nabla F}{\sqrt{1+\lambda_F|\nabla F|^2}}. \tag{11}$$

Macrophages are recruited from Th1 cells through cytokines such as IFN-γ and TNF-α, and this recruitment can be inhibited by Th2 cell secreted cytokines such as IL-4 or IL-5 (Figure 3). Macrophages may also undergo *apoptosis* with a death rate μ_M. Taking into account these observations, we get the production/death term

$$P_M = \frac{\lambda_{13}FH_1}{\lambda_{14}^l + I_1^l}M\left(1-\frac{M}{K_3}\right) - \mu_M M \tag{12}$$

where λ_{13} is the rate of production of macrophages and λ_{14} is the inhibition parameter for the creation of macrophages with the Hill-type coefficient l.

In summary, we have the following form for the macrophage density:

$$\frac{\partial M}{\partial t} = \underbrace{D_M\Delta M}_{\text{Random motility}} \underbrace{-\nabla\cdot\left(\chi\frac{M\nabla F}{\sqrt{1+\lambda_F|\nabla F|^2}}\right)}_{\text{chemotaxis}} + \underbrace{\frac{\lambda_{13}FH_1}{\lambda_{14}^l + I_1^l}M\left(1-\frac{M}{K_3}\right)}_{\text{production}} - \underbrace{\mu_M M}_{\text{death}}. \tag{13}$$

2.5. **IFN-γ concentration (=$F(x,t)$).** The mass balance equation for IFN-γ is

$$\frac{\partial F}{\partial t} + \nabla\cdot J = P_F \tag{14}$$

where J is the flux of IFN-γ and P_F is the production/decay term. The only contribution to the flux J is the diffusion process leading to the flux

$$J = -D_F\nabla F, \tag{15}$$

where D_F is the diffusion coefficient of IFN-γ. IFN-γ is secreted by Th1 cells [61] (Figure 3) and undergoes natural decay, leading to

$$P_F = \lambda_1 H_1 - \mu_F F, \tag{16}$$

where λ_1 is the production rate of IFN-γ from Th1 cells and μ_F is the decay rate. In summary, the governing equation for IFN-γ concentration is

$$\frac{\partial F}{\partial t} = \underbrace{D_F\Delta F}_{\text{Diffusion}} + \underbrace{\lambda_1 H_1}_{\text{production}} - \underbrace{\mu_F F}_{\text{decay}}. \tag{17}$$

2.6. **IL-4 concentration (=$I_1(x,t)$).** This cytokine, IL-4, is secreted by Th2 cells [9] and helps the development of Th2 cells (Figure 3). Using the mass balance equation for the IL-4 concentration with the flux J due to the diffusion process, similar to the equation (14) above, we derive the following governing equation for the IL-4 concentration

$$\frac{\partial I_1}{\partial t} = \underbrace{D_{I_1}\Delta I_1}_{\text{Diffusion}} + \underbrace{\lambda_3 H_2}_{\text{production}} - \underbrace{\mu_{I_1} I_1}_{\text{decay}}, \tag{18}$$

where D_{I_1} is the diffusion coefficient of IL-4, λ_3 is the production rate of IL-4 from Th2 cells, and μ_{I1} is the decay rate of IL-4.

2.7. **IL-12 concentration (=$I_2(x,t)$).** IL-12 is produced by Th1 cells [70] and macrophages [42]. It has been shown that high doses of LPS induce enhanced IL-12 expression during allergen sensitization [53]. In this context, we assume that the production of IL-12 from Th1 cells is dependent on the LPS dose ($\alpha = \alpha(t)$) and take a Hill type function with the coefficient n. In our model, this LPS input level (α) is a key control parameter. These considerations lead to a mass balance equation for IL-12 concentration

$$\frac{\partial I_2}{\partial t} = \underbrace{D_{I_2}\Delta I_1}_{\text{Diffusion}} + \underbrace{\frac{\lambda_8 \alpha(t)^n}{\lambda_9^n + \alpha(t)^n} H_1 + \lambda_{10} M}_{\text{production}} - \underbrace{\mu_{I_2} I_2}_{\text{decay}}, \tag{19}$$

where D_{I_2} is the diffusion coefficient of IL-12, λ_8 is the rate of IL-12 production from Th1 cells, λ_{10} is the rate of IL-12 production from macrophages, and μ_{I2} is the decay rate of IL-12.

2.8. **TNF-α concentration (=$T(x,t)$).** TNF-α is mainly produced by macrophages [12, 93] while other cells such as lymphoid cells and mast cells may produce this cytokine. Both Th1 and Th2 synthesize TNF-α [70]. In the experiments in [53], TNF-α levels were significantly higher in wild type with OVA plus LPS doses than in those without the LPS treatment. Here we assume that TNF-α is secreted by Th1 cells, Th2 cells, and macrophages. Then the governing equation for TNF-α becomes

$$\frac{\partial T}{\partial t} = \underbrace{D_T \Delta T}_{\text{Diffusion}} + \underbrace{\lambda_4 H_1 + \lambda_{11} H_2 + \lambda_{12} M}_{\text{production}} - \underbrace{\mu_T T}_{\text{decay}}, \tag{20}$$

where D_T is the diffusion coefficient of TNF-α, μ_T is the decay rate of TNF-α, and $\lambda_4, \lambda_{11}, \lambda_{12}$ are the rates of TNF-α secretion from Th1 cells, Th2 cells, and macrophages, respectively.

2.9. **Governing equations.** In summary, a system of governing equations of all variables ($H_1(x,t)$, $H_2(x,t)$, $H_0(x,t)$, $M(x,t)$, $F(x,t)$, $I_1(x,t)$, $I_2(x,t)$, $T(x,t)$) in

the domain Ω is described by

$$\begin{aligned}
\frac{\partial H_1}{\partial t} &= D_{H_1}\Delta H_1 + \frac{\lambda_5 I_2}{\lambda_6^m + I_1^m} H_0 H_1 \left(1 - \frac{H_1}{K_1}\right) - \mu_{H_1} H_1,\\
\frac{\partial H_2}{\partial t} &= D_{H_2}\Delta H_2 + \frac{\lambda_2 T I_1}{\lambda_7^k + F^k} H_0 H_2 \left(1 - \frac{H_2}{K_2}\right) - \mu_{H_2} H_2,\\
\frac{\partial H_0}{\partial t} &= D_{H_0}\Delta H_0 + \beta - \left(\frac{\lambda_5 I_2}{\lambda_6^m + I_1^m} H_0 H_1 + \frac{\lambda_2 T I_1}{\lambda_7^k + F^k} H_0 H_2\right) - \mu_{H_0} H_0,\\
\frac{\partial M}{\partial t} &= D_M \Delta M - \nabla \cdot \left(\chi \frac{M \nabla F}{\sqrt{1 + \lambda_F |\nabla F|^2}}\right) + \frac{\lambda_{13} F H_1}{\lambda_{14}^l + I_1^l} M \left(1 - \frac{M}{K_3}\right) - \mu_M M,\\
\frac{\partial F}{\partial t} &= D_F \Delta F + \lambda_1 H_1 - \mu_F F,\\
\frac{\partial I_1}{\partial t} &= D_{I_1}\Delta I_1 + \lambda_3 H_2 - \mu_{I_1} I_1,\\
\frac{\partial I_2}{\partial t} &= D_{I_2}\Delta I_1 + \frac{\lambda_8 \alpha^n}{\lambda_9^n + \alpha^n} H_1 + \lambda_{10} M - \mu_{I_2} I_2,\\
\frac{\partial T}{\partial t} &= D_T \Delta T + \lambda_4 H_1 + \lambda_{11} H_2 + \lambda_{12} M - \mu_T T.
\end{aligned} \tag{21}$$

Boundary conditions:

The boundary ($\partial\Omega$) of the computational domain (Ω) consists of two disjointed subsets, Γ_1, Γ_2, *i.e.*, $\partial\Omega = \Gamma_1 \cup \Gamma_2, \Gamma_1 \cap \Gamma_2 = \emptyset$. Macrophages are provided from blood vessels and we prescribe the *Dirichlet* (fixed) boundary condition on a portion of boundary (Γ_1) near the blood vessel. We also assume that there is no flux on the other boundary Γ_2 (*Neumann* B.C.).

$$M = M_0, \quad \text{on } \Gamma_1 \tag{22}$$

$$\nu \cdot \left(D_M \nabla M - \chi \frac{M \nabla F}{\sqrt{1 + \lambda_F |\nabla F|^2}}\right) = 0, \text{ on } \Gamma_2, \tag{23}$$

where ν is the outer normal vector and M_0 is the fixed macrophage density on Γ_1. No flux boundary conditions (*Neumann*) were applied for all other variables on the whole boundary ($\partial\Omega = \Gamma_1 \cup \Gamma_2$):

$$\begin{aligned}
&\nu \cdot (D_{H_1} \nabla H_1) = 0, \ \nu \cdot (D_{H_2} \nabla H_2) = 0, \ \nu \cdot (D_{H_0} \nabla H_0) = 0,\\
&\nu \cdot (D_F \nabla F) = 0, \ \nu \cdot (D_{I_1} \nabla I_1) = 0, \ \nu \cdot (D_{I_2} \nabla I_2) = 0, \qquad \text{on } \partial\Omega\\
&\nu \cdot (D_T \nabla T) = 0.
\end{aligned} \tag{24}$$

Initial conditions would be described for the local dynamics (ODE) and full dynamics (1D or 2D PDE) in the corresponding subsections below. In the next Section, we present the results of the model.

3. Results.

In the following section, we first describe the local dynamics of the mathematical model and compare some of the computational results to experimental results from [53].

3.1. Local dynamics.

Figure 4 shows a typical time course of densities of cells (Th1 cells (H_1), Th2 cells (H_2), and Th0 cells (H_0)), and concentrations of regulating factors (IFN-γ (F), IL-4 (I_1), IL-12 (I_2), and TNF-α (T)) when low doses of LPS ($\alpha = 1.0$) were used. Th2 cells become dominant along with high levels of IL-4

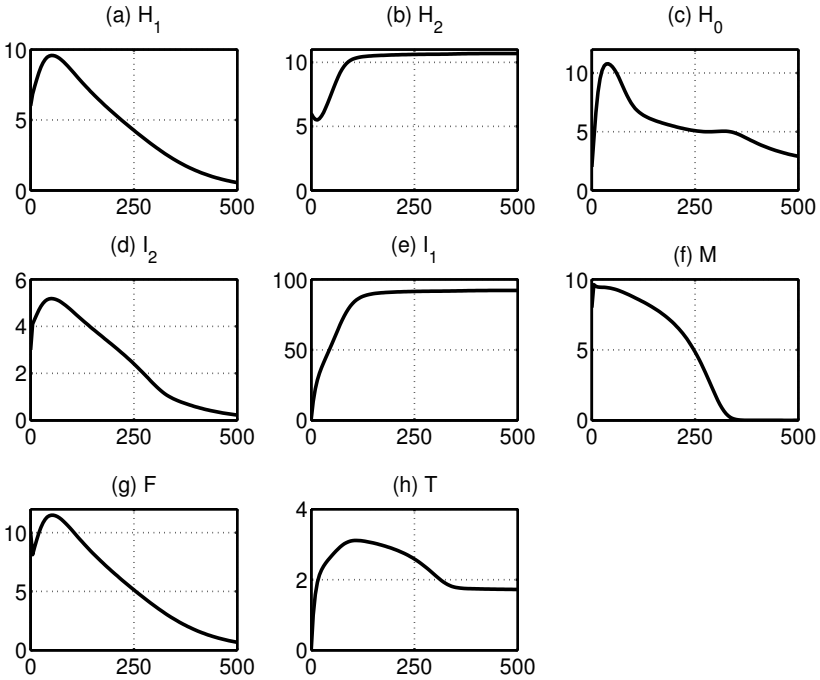

FIGURE 4. A time course of all variables in response to low doses of LPS: Densities of Th1 cells ($H_1(t)$), Th2 cells ($H_2(t)$), Th0 cells ($H_0(t)$), macrophages, and concentrations of IFN-γ ($F(t)$), IL-4 ($I_1(t)$), IL-12 ($I_2(t)$), and TNF-α (T). The local dynamic model (ODEs) was used for the simulation with low levels of LPS ($\alpha = 1.0$). The low dose LPS leads to the Th2-dominant system, *i.e.,* increases in Th2 population and IL4 levels, and decreases in populations of Th1 cells and macrophages, and concentrations of IL-12 and IFN-γ. Initial conditions: $H_1(0) = 6.0, H_2(0) = 6.0, H_0(0) = 2.0, M(0) = 8.0, F(0) = 10.0, I_1(0) = 1.0, I_2(0) = 3.0, T(0) = 0.01$.

while the populations of Th1 cells and macrophages as well as levels of their associated molecules (IL-12 and IFN-γ) are decreased. The low LPS level ($\alpha = 1$) led to low proliferation of Th1 cells and low IFN-γ secretion from Th1 cells. Low levels of IL-12 follow due to small contributions from Th1 cells. Low levels of IFN-γ also weaken the inhibitory action against Th2 proliferation, leading to the faster conversion from naive Th0 cells to Th2 cells. This increase in the number of Th2 cells leads to an increase in secretion of IL-4, which further counteracts the conversion of Th0 cells to Th1 cells. On the other hand, the macrophage population is getting smaller due to lowered positive contributions from IFN-γ levels and Th1 cells, and increased inhibitory effects from higher IL-4 levels (I_1). The small population of macrophages also generates small contributions toward IL-12 (I_2), enhancing the Th2-IL-4 cycle. We found that the overall model behavior of all variables for low levels of LPS ($\alpha < 1.0$) is quantitatively similar to ones when $\alpha = 1$, which is also consistent with experimental data in [53].

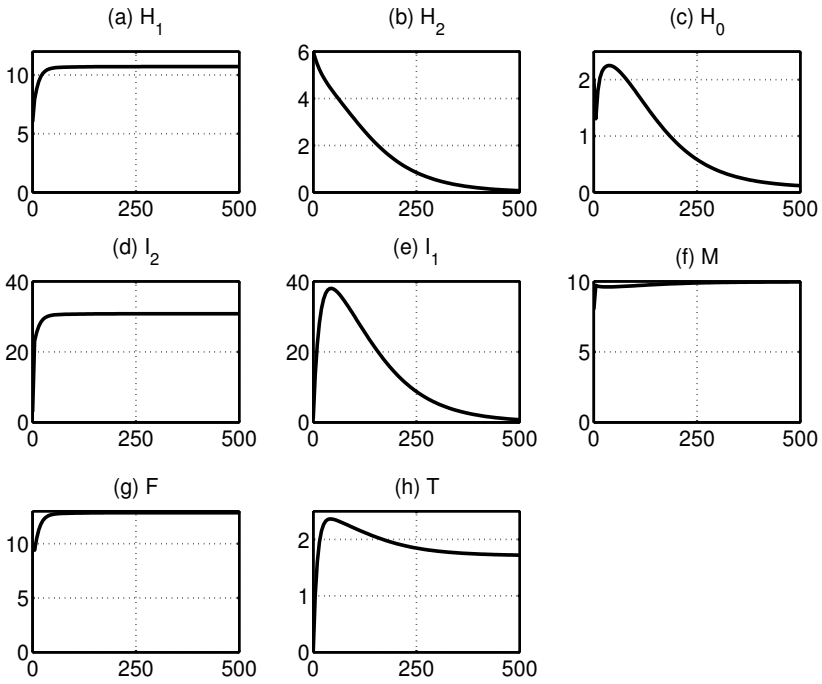

FIGURE 5. A time course of all variables in response to high doses of LPS: Densities of Th1 cells ($H_1(t)$), Th2 cells ($H_2(t)$), Th0 cells ($H_0(t)$), macrophages, and concentrations of IFN-γ ($F(t)$), IL-4 ($I_1(t)$), IL-12 ($I_2(t)$), and TNF-α (T). The local dynamics (ODEs) was used for the simulation with high levels of LPS input (α=100.0). The high dose LPS leads to the Th1-dominant system, *i.e.,* increases in populations of Th1 cells and macrophages, and levels of IL-12 and IFN-γ, and decreases in Th2 cells and IL-4 levels. Initial conditions: $H_1(0) = 6.0$, $H_2(0) = 6.0$, $H_0(0) = 2.0$, $M(0) = 8.0$, $F(0) = 10.0$, $I_1(0) = 1.0$, $I_2(0) = 3.0$, $T(0) = 0.01$.

Figure 5 shows a typical time course of densities of all variables when the LPS input (α=100.0) is large. Th1 cells become dominant as shown in the experiment [53]. While high levels of population densities of Th1 cells and macrophages, and concentrations of IL-12 and IFN-γ were observed, Th2 cell populations and IL-4 levels are decreased. The high dose of LPS leads to large contributions toward IL-12 (I_2) levels and elevated levels of IL-12 then enhance the cell conversion from Th0 to Th1 type, increasing IFN-γ secretion from Th1 cells and enhancing IL-12 secretion. This high IFN-γ level strengthens the inhibition of cell conversion from the Th0 to Th2 subtype and enhances macrophage proliferation along with increased Th1 cell numbers. The system with the large number of macrophages also induces IL-12 secretion. The population of Th2 cells is decreased due to these positive feedback loops among IL-12, Th1 cells, IFN-γ, and macrophages. This leads to low IL-4 levels (I_1), which further suppresses Th2 cell proliferation and the inhibitory action against the population of Th1 cells. As shown in the experiment in [53], TNF-α (T) expression was enhanced by both low- and high-dose LPS (α=10,100), while

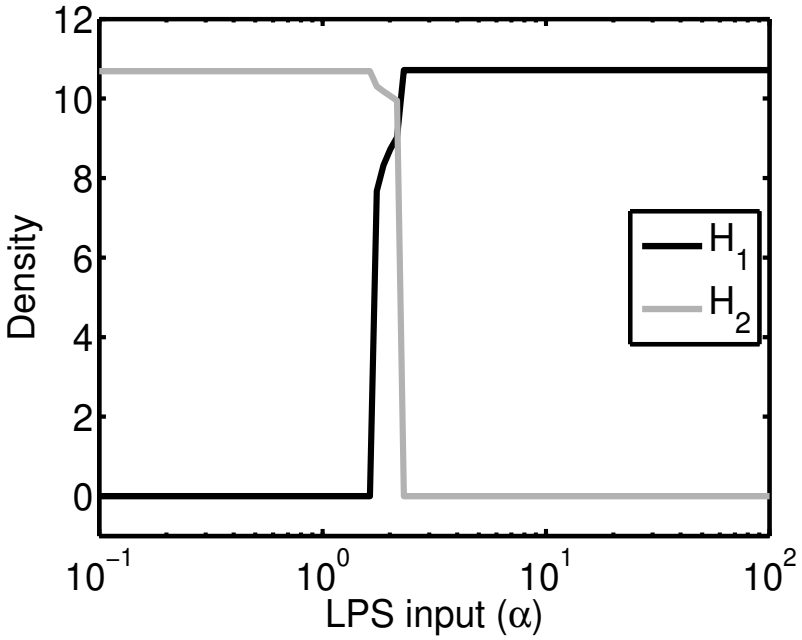

FIGURE 6. Steady state values of Th1 (black) and Th2 (gray) populations as functions of the LPS injection level (α). As the LPS level (α) is increased, the inflammatory reaction switches from Th2 cell induced asthma (α=0.1) to Th1 cell induced asthma (α=100.0). It also suggests coexistence of those distinct subtypes (Th1/Th2) and the emergence of third phenotype. Initial conditions: $H_1(0) = 6.0, H_2(0) = 6.0, H_0(0) = 2.0, M(0) = 8.0, F(0) = 10.0, I_1(0) = 1.0, I_2(0) = 3.0, T(0) = 0.01$.

IL-12 expression (I_2) was only enhanced by the high-dose LPS (α=10,100) during the allergen sensitization period (see Figures 4,5). We also note that the model system for relatively high LPS levels (α=10-100) show the same behavior as one for the very high LPS level (α=100).

Figure 6 shows the populations of Th1 and Th2 cells as a function of the LPS input level (α). As experimentally shown in [53], a Th2-dominant system can switch to the Th1-dominant system as the LPS level (α) is increased. It also predicts that there exists a narrow area [1.2, 2.4] of LPS levels for the coexistence of Th1/Th2 subtypes, predicting the emergence of a third phenotype, Th17 [41], for intermediate levels of LPS.

3.2. **Full dynamics.** All the simulations in this section were performed using a finite volume method and *clawpack* (http://depts.washington.edu/clawpack/) with a fractional step method [100] as well as the non-linear solver *nksol* for algebraic systems. The equations (4)-(20) are solved on a regular uniform spatial grid (Δx=0.01). An initial time step of $\Delta t = 1.0 \times 10^{-6}$ was used, but adaptive time stepping based on the number of iterations did alter this step size.

First, we investigated the effect of LPS levels on Th1/Th2 regulation in asthma with the one-dimensional setup. The computational domain is $\Omega = [0, 1]$. Differential localization of Th1 and Th2 cells was observed in autoimmune gastritis [49]. Alternative waves were used to describe the initial conditions of those two competing phenotypes, Th1 cells (H_1) and Th2 (H_2). We prescribe a uniform distribution of the source phenotype, Th0 cells (H_0). Macrophages are assumed to be initially localized on the lefthand side ($x = 0$) of the computation domain near blood vessels. We take uniform distributions of regulating molecules, IFN-γ (F), IL-4 (I_1), IL-12 (I_2) and TNF-α (T). The following initial conditions were used for the one-dimensional case:

$$\begin{aligned} &H_1(x,0) = 6.0 * (\sin(8.0\pi x) + 1),, \ H_2(x,0) = 6.0 * (-\sin(8.0\pi x) + 1), \\ &H_0(x,0) = 2.0, \ M(x,0) = 10.0\exp(-50x), \ F(x,0) = 10.0, \\ &I_1(x,0) = 1.0, \ I_2(x,0) = 3.0, \ T(x,0) = 0.02. \end{aligned} \tag{25}$$

Figure 7 shows a time course of populations of cells and levels of regulating molecules in response to high (α=10; black dotted line) and low (α=0.1, 1.0) levels of LPS: Th1 cells ($\hat{H}_1$ in (A)), Th2 cells ($\hat{H}_2$ in (B)), Th0 cells ($\hat{H}_0$ in (C)), and macrophages ($\hat{M}$ in (D)), and levels of IFN-γ ($\hat{F}$ in (E)), IL4 ($\hat{I}_1$ in (F)), IL-12 ($\hat{I}_2$ in (G)), TNF-α ($\hat{T}$ in (H)). Here, populations and concentrations denoted by a hat ($\wedge$) were obtained by taking an integration over the domain (Ω). For example, $\hat{H}_1(t) = \int_\Omega H_1(x,t)dx$. Overall behaviors of the system in response to high and low LPS levels are similar to those in local dynamics, *i.e.,* low doses of LPS favor the Th2 phenotype while high doses of LPS lead to the Th1-dominant system. One can also notice a slow transition from Th2 cell induced asthma to Th1 cell induced asthma as the LPS level (α) is increased. For instance, it takes a long time to get the small population of macrophages when $\alpha = 1$ while the lower LPS level ($\alpha = 0.1$) leads to an immediate decrease in the macrophage population.

Figure 8 illustrates how LPS levels can increase or decrease levels of IL-12. In the experiments in [53], IL-12 levels are low ($\sim 210 - 500\ pg/ml$) for low LPS input levels (0.1, 1 μg) after allergen sensitization while high doses of LPS (10, 100 μg) can induce high levels of IL-12 ($\sim 1,100\ pg/ml$) (see Figure 8A). Levels of this Th1-associated cytokine, IL-12, are also reduced in low LPS (α=0.1, 0.2, 0.3, 1) and high for elevated doses of LPS ($\alpha = 10, 100$) in our model (Figure 8). See Figure 8B. While the experiments were not performed for intermediate levels of LPS (1-10 μg) in [53], the model predictions indicate these conditions would lead to intermediate IL-12 levels (α=2,5 in Figure 8B).

In Figure 9 we investigated the dynamics of the macrophage population in response to various LPS levels (α=0.1, 0.2, 0.3, 1, 3, 100). Macrophage infiltration was high when LPS levels were high and a small population of macrophages was observed when small amounts of LPS were used in the experiments [53] (Figure 9A). Our simulation predicted the consistent results, *i.e.,* the population of macrophages is an increasing function of the LPS level (α) as predicted in the experiments in [53] (Figure 9B).

Figure 10 shows that the secretion of IL-4 enhanced by low doses of LPS ($\alpha = 0.1, 1$) in wild type (WT) was not observed in the mutant, but there were not significant differences in IL-4 secretion rates between the wild type and its mutant. Consistent experimental results were illustrated in [53] using TNFR1-deficient ($\text{TNFR1}^{(-/-)}$) and WT mice sensitized with high- (10 μg) and low-dose (0.1 μg)

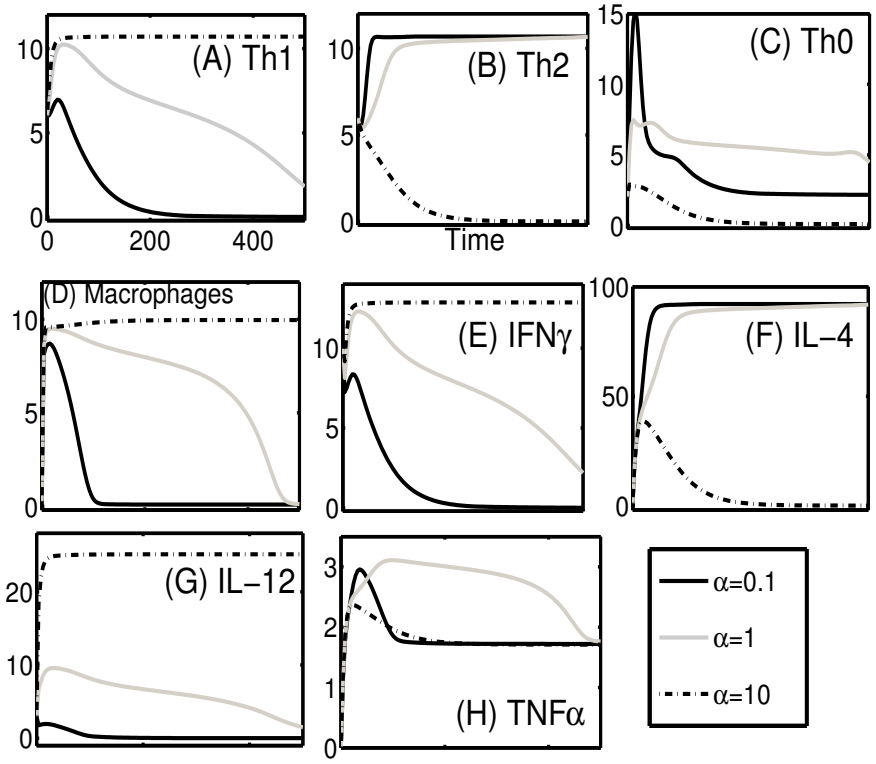

FIGURE 7. A time course of populations of cells and concentrations of regulating molecules for various LPS levels ($\alpha = 0.1, 1, 10$): (A) population of Th1 cells ($\hat{H}_1$) (B) population of Th2 cells ($\hat{H}_2$) (C) population of Th0 cells ($\hat{H}_0$) (D) population of macrophages ($\hat{M}$), (E) level of IFN-γ ($\hat{F}$) (F) level of IL-4 ($\hat{I}_1$) (G) level of IL-12 ($\hat{I}_2$) (H) level of TNF-α ($\hat{T}$) in the one-dimensional model. Low levels of LPS ($\alpha = 0.1, 1$) induce Th2-dominant phase. The high dose LPS ($\alpha = 10$)promotes Th1 cells, macrophages, and their associated molecules (IFN-γ, IL-12). Here, populations of cells and levels of chemicals denoted by a hat ($\wedge$) were obtained by taking an integration over the domain (Ω), *i.e.*, $\hat{u}(t) = \int_\Omega u(x,t)dx$. Time scales in (B)-(H) are same as one in (A).

LPS. For example, IL-4 levels were significantly reduced in both simulations (∼60%) and experiments (∼68%) in [53], when a low level of LPS ($\alpha = 0.1$ in the simulation; $0.1\mu g$ in [53]) was injected. On the other hand, no significant differences were found in the case of high-dose LPS ($\alpha = 10$ in the simulation; $10\mu g$ in [53]) in both simulation (∼16% reduction) and experiments (∼5% reduction [53]). For the TNFR1$^{(-/-)}$ case, much lower TNF-α secretion rates ($\frac{\lambda_4}{100}, \frac{\lambda_{11}}{100}, \frac{\lambda_{12}}{100}$) were used in the simulations.

In Figure 11, we investigated the effect of IFN-γ-knockdown (IFN-$\gamma^{-/-}$) on the population of macrophages for a high dose of LPS ($\alpha = 10$). In the experiments in [53], airway infiltration of macrophages after allergen challenge did not develop in IFN-γ-deficient (IFN-$\gamma^{-/-}$) mice sensitized with OVA plus high-dose LPS (10

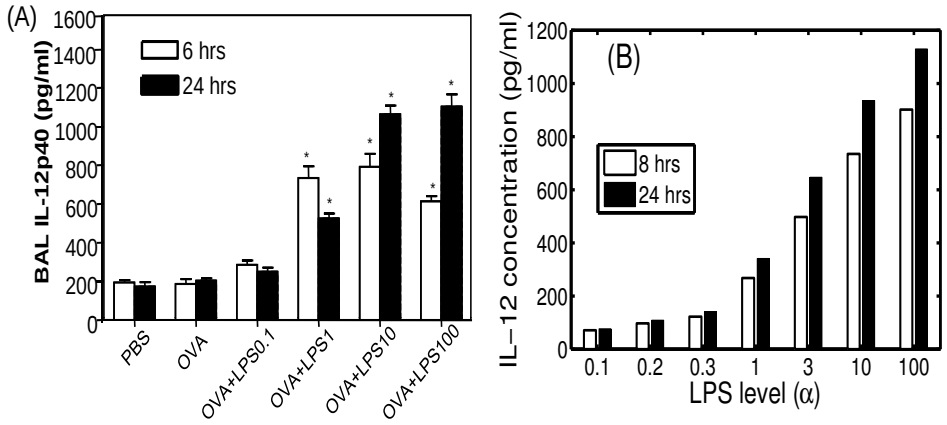

FIGURE 8. Regulation of IL-12 in response to high and low LPS. (A) Experimental observation: High levels of LPS (10, 100 μg) up-regulated IL-12p40 levels 6 and 24 h after allergen sensitization but low-dose (0.1 μg) LPS did not increase IL-12p40 production. The figure from Kim *et al.* [53] with permission. (B) Simulation results: IL-12 concentration for various LPS levels at $t = 8h, 24h$. IL-12 levels were up-regulated by high doses of LPS but not by low doses of LPS.

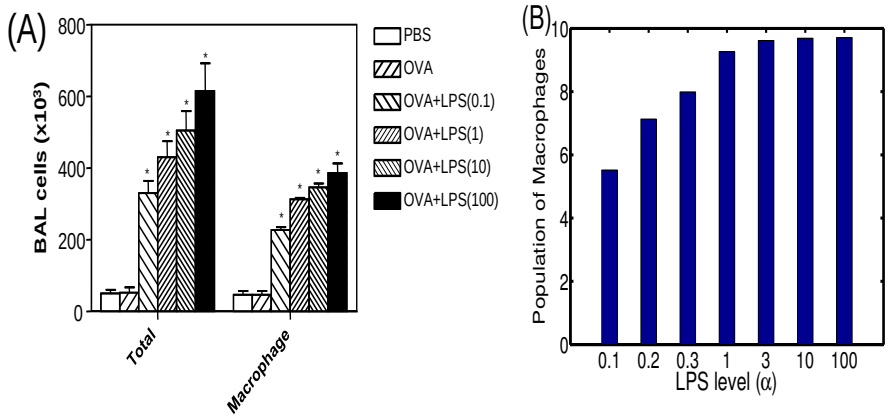

FIGURE 9. Population of macrophages in response to various LPS levels. (A) Population of macrophages for different LPS values (0.1, 1, 10, 100 μg) in experiments (Figure 3B in [53] ; BAL cellularity after allergen challenge: bar heights represent cell numbers of total cells and macrophages). The figure from Kim *et al.* [53] with permission. (B) Simulation results: The population of macrophages is increased as LPS input levels (α) are increased.

μg) relative to wild type (WT) mice. The simulation results also show that the macrophage population is significantly decreased in response to high-dose LPS (73% and 67% reductions for $\alpha = 10, 100$, respectively) in the IFN-γ knock-down case relative to WT. A low level or absence of IFN-γ (F) directly reduces the proliferation potential of macrophages (equation (13)). The lowered level of IFN-γ also increases

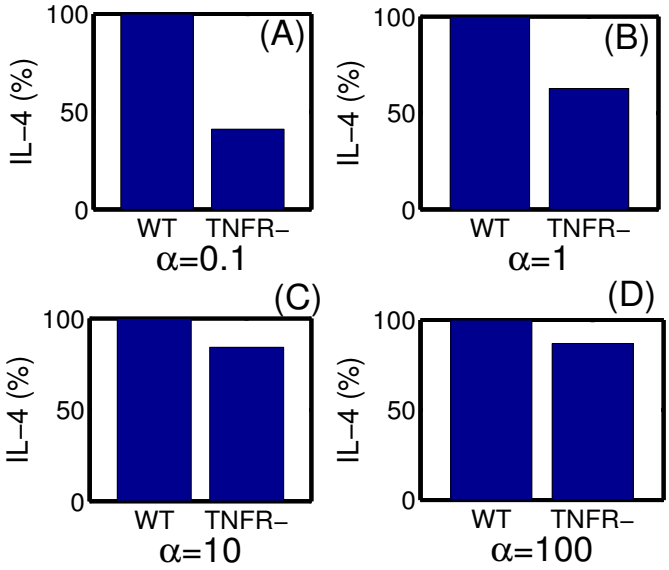

FIGURE 10. IL-4 levels for wild type (WT) and TNF-α mutant (TNFR-) after allergen challenge for various LPS levels (α). IL-4 enhancements by low doses of LPS ($\alpha = 0.1, 1$) were inhibited in the absence of TNFR1 gene (TNFR1$^{(-/-)}$) while IL-4 productions induced by high doses of LPS ($\alpha = 10, 100$) were not.

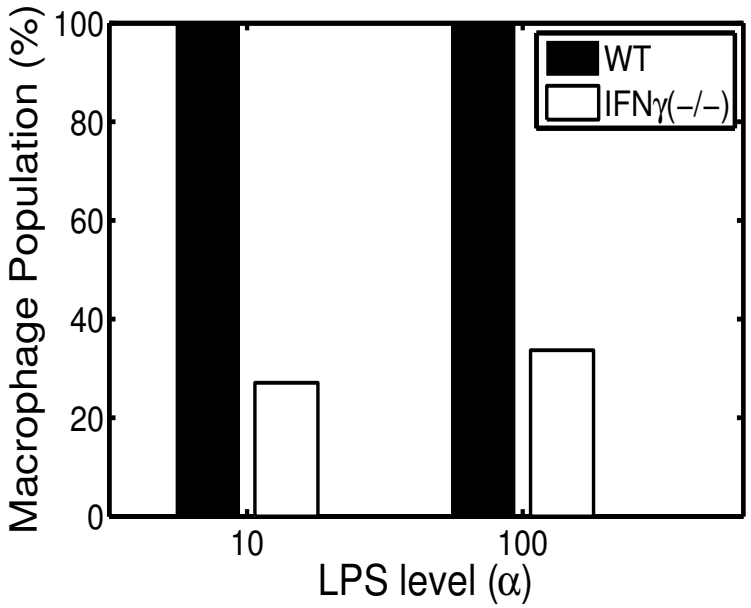

FIGURE 11. Macrophage population in response to high doses of LPS ($\alpha = 10, 100$) in the wild type (WT) and IFN-γ knockdown case (IFN-$\gamma^{-/-}$). The macrophage population is significantly decreased (73% and 67% reductions for $\alpha = 10, 100$, respectively) in IFN-$\gamma^{-/-}$ relative to WT (*cf.* Figure 6B in [53]).

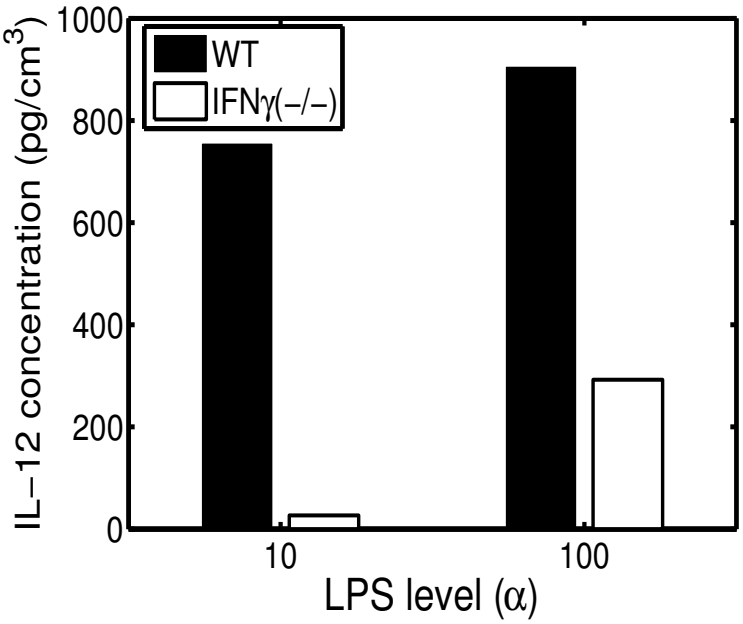

FIGURE 12. IL-12 level for wild type (WT) and IFN-γ knockdown case (IFN-$\gamma^{-/-}$) with high-dose LPS (α). IL-12 concentration is significantly reduced (94% and 68% reductions for $\alpha = 10, 100$, respectively) for IFN-γ knockdown (IFN-$\gamma^{-/-}$), compared to WT in both experiments [53] and simulations. (*cf* Figure 6D in [53]).

the Th2 population indirectly due to the reduction of its inhibitory effect on Th2 proliferation (in equation (6)), which leads to the increased IL-4 (I_1) secretion by Th2 cells (H_2) (in equation (17)) and the promotion of inhibitory effect on growth of macrophage population (equation (13)). These direct and indirect regulations induce the decreased population of macrophages. Kim *et al.* [53] found that the absence of IL-4 did not affect this cellularity enhanced by high-dose LPS (10 μg) in IL-4-deficient ($^{-/-}$) mice. Simulation results indicate that the knockdown of IL-4 with a high LPS level ($\alpha = 10$) does not affect the macrophage population (data not shown).

Figure 12 shows that this IFN-γ knockdown (IFN-$\gamma^{-/-}$) with high-dose LPS ($\alpha = 10$) induces reduction in IL-12 secretion. In the wild type, high levels of LPS induce high levels of IL-12 both directly through LPS, and indirectly via the increased population of Th1 cell types (in equation (19)) as shown in Figure 5 and discussions above. However, a low level or absence of IFN-γ weakens its inhibitory effect on the population of Th2 cells and induces a decrease in the macrophage population as discussed above. This leads to a reduction of IL-12 levels due to decreased contributions from the macrophage population. IL-12 secretion from Th1 cells is also reduced due to the Th2-dominant system. These two negative factors overcome the positive contributions from high LPS levels and the IL-12 level overall is decreased in the IFN-$\gamma^{-/-}$ case despite high LPS levels. The experimental data from the high-dose (10 μg) LPS-enhanced asthma model using the IFN-γ-deficient mouse support these computational results (Figure 6D in [53]). So, the

experiments and our computational model suggest that IFN-γ is one of the key players in regulating type I and II asthma in response to various LPS levels (α) and plays a significant role in developing AHR and noneosinophilic lung inflammation in high-dose LPS.

In the following, we investigated the role of the microenvironment in the regulation of type I and II asthma in response to various levels of LPS using our computational model in a two-dimensional (2D) setup. In order to predict possible behaviors of the key players, Th1 and Th2 cells, in a perturbed system, those two subtypes are assumed to have very different initial configurations. A Th1 cell aggregate was localized at the center (0.5,0.5) of the computational domain $\Omega = [0,1] \times [0,1]$ and many smaller Th2 cell aggregates were placed on a spiral track originating from the center of the domain Ω. We used the following initial conditions of Th1 (H_1) and Th2 cells (H_2) with the same initial conditions for other variables (Th0 cells (H_0), IFN-γ (F), IL-4 (I_1), IL-12 (I_2), TNF-α (T)):

$$\begin{aligned} H_1(x,y,0) &= 12 * \exp[-50 * ((x-0.5)^2 + (y-0.5)^2)]), \\ H_2(x,y,0) &= \sum_{j=1}^{N_p} 12 \exp[-200 * ((x-p_x^j)^2 + (y-p_y^j)^2)], \\ H_0(x,y,0) &= 2.0, \\ M(x,y,0) &= 10 \exp(-50x), \\ F(x,y,0) &= 10, \\ I_1(x,y,0) &= 1.0, \\ I_2(x,y,0) &= 3.0, \\ T(x,y,0) &= 0.01, \end{aligned} \tag{26}$$

where $(p_x^j, p_y^j) = (0.5 + d_j \cos(\theta_j), 0.5 + d_j \sin(\theta_j))$ $(j = 1, \ldots, N_p)$ are center points of spherical Th2 cell aggregates, $\theta_j = \frac{(j-1)*2\pi}{N_p}$, $(j = 1, \ldots, N_p)$, $d_1 = 0.1$, $d_{N_p} = 0.4$, $d_j = \frac{(d_{N_p} - d_1)*(j-1)}{(N_p - 1)} + d_1$, $(j = 2, \ldots, N_p - 1)$, $N_p = 8$.

In Figure 13, we show different spatial patterns of density profiles of Th1 cells, Th2 cells, and macrophages for various levels of LPS ($\alpha = 0.1, 3, 10$). To see the effects of different microenvironment on regulation of type I and II asthma, different diffusion coefficients of molecules and random motility of cells were used in the left ($\Omega_1 = [0, 0.5] \times [0, 1]$) and right ($\Omega_1 = [0.5, 1] \times [0, 1]$) half of the computational domain (Ω). When low-dose LPS ($\alpha = 0.1$) was introduced, Th2 cells on a spiral track quickly spread and proliferate to become a dominant phenotype after $t = 200$. Th1 cells and macrophages sustain the populations at the center of the domain but their growth is eventually suppressed and the populations die out. See Figure 13A. In the case of high-dose LPS ($\alpha = 10$; Figure 13C), Th1 cells quickly spread across the domain and suppress Th2 cell types except a relatively small island on the left side of the domain. Abundant macrophages also help Th1 cells by secreting IL-12. For an intermediate level of LPS ($\alpha = 3.0$), the patterns show co-existence of both phenotypes (Th1 cells and Th2 cells). One can note that these patterns of Th1 cells and Th2 cells for the intermediate LPS level may depend on many factors such as initial distributions of cell populations and chemicals as well as random motility of cells and diffusivity of chemicals as shown below in Figure 14. One also observes that different spreading speeds of those populations on the left

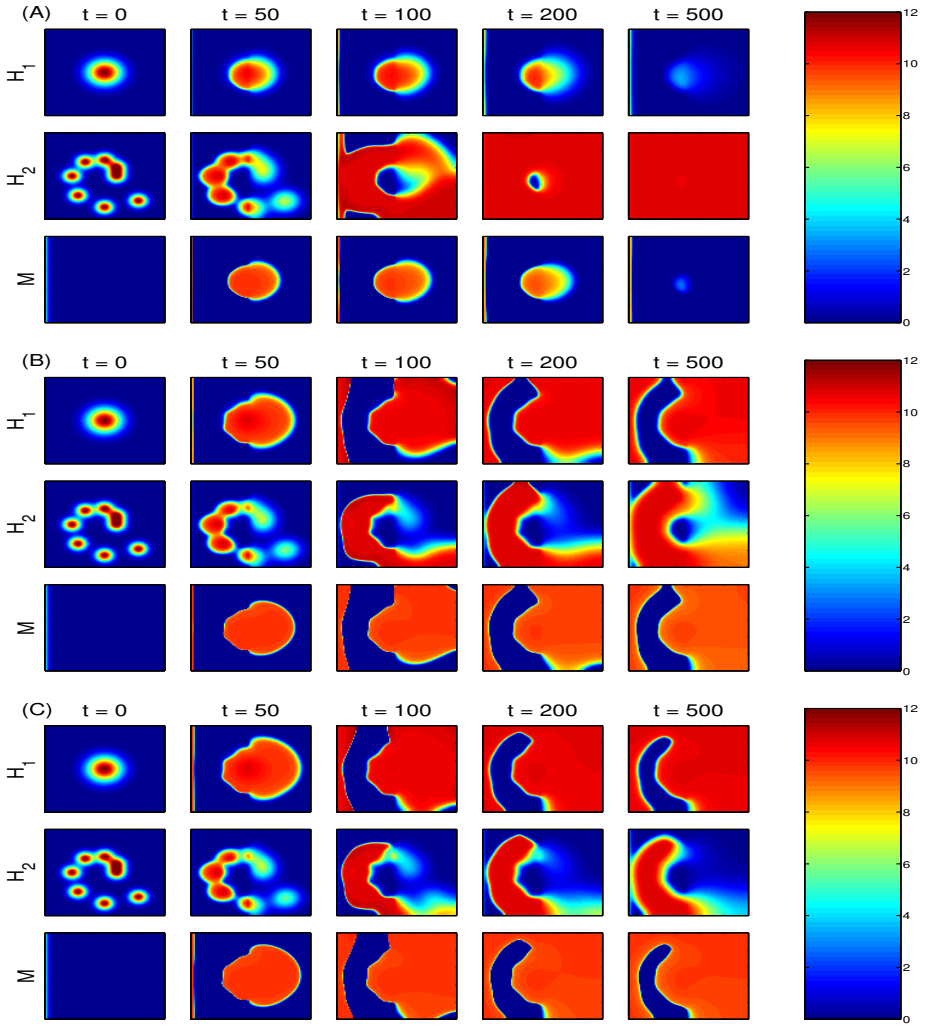

FIGURE 13. A time course of profiles of Th1 cells, Th2 cells, and macrophages for various LPS levels: (A) low LPS level ($\alpha = 0.1$) (B) intermediate LPS level ($\alpha = 3$) (C) high LPS level ($\alpha = 10$). For low LPS input, Th2 cells become a dominant cell type. In contrast, high LPS levels induce Th1-dominant phases. We also observe the wild spread of macrophages. For intermediate levels of LPS, mixed populations of Th1 and Th2 cells are observed. Initially, Th1 cells were localized at the center (0.5,0.5) of the the 2D computational domain (Ω) while eight Th2 cell aggregates were placed on a spiral track Γ originated from the center of the domain. Normal diffusion coefficients were assigned on the right half of the domain (Ω_2) while smaller diffusion coefficients were assigned on the left half (Ω_2). (See the main context for more detail.) The computational domains: $\Omega = [0,1] \times [0,1]$, $\Omega_1 = [0, 0.5] \times [0,1]$, $\Omega_2 = [0.5, 1] \times [0,1]$. Grid size 100×100.

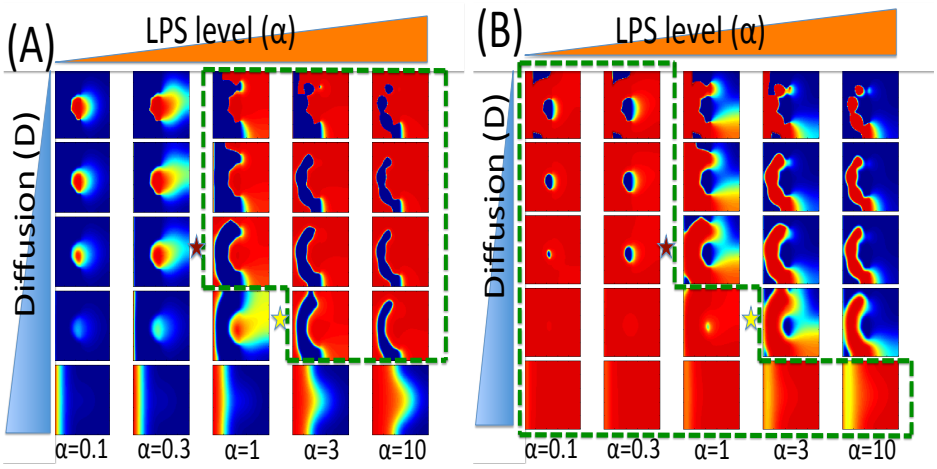

FIGURE 14. Role of the microenvironment in regulation of T cell responses. Profiles of two competing phenotypes (Th1 cells in (A) and Th2 cells in (B)) in $\alpha - D_L$ plane at final time ($t = 500$), where D_L represents the diffusion coefficients of chemicals or random motility of cells on the left half domain ($\Omega_1 = [0, 0.5] \times [0, 1]$). Normal diffusion coefficients (D_R) of all variables were assigned on the right half domain (Ω_2) while various diffusion coefficients ($D_L^i =$ i-th row ($i = 1, \ldots, 5$); $D_L^1 < D_L^2 < D_L^3 < D_L^4 < D_L^5$) were assigned for all variables on the left half of the domain ($\Omega_1 = [0.5, 1] \times [0, 1]$). In each column, different LPS levels ($\alpha = 0.1, 0.3, 1, 3, 10$) were used. Initial conditions of all variables and colorbar are same as in Figure 13, *i.e.,* red= high density, blue= low density. Dominant phenotypes (red) were enclosed by the green dotted line in (A) and (B). Th1 cells become a dominant cell type as the LPS level (α) is increased. When the tissue becomes stiffer and diffusion rates are low, Th1 cells become dominant even for low LPS levels ($\alpha = 1.0$; 3rd row). A LPS threshold value α^{th} for separating type I asthma from type II asthma was marked in star (brown star in 3rd row and yellow star in 4th row). This threshold value α^{th} is decreased as tissue becomes stiffer (from yellow star to brown star), *i.e.,* the diffusion coefficients and random motilities are decreased.

(Ω_1) and right (Ω_2) half of the domain (Ω). Th2 cells benefit from local dynamics instead of spreading (the survived island for $\alpha = 10$ for instance). Therefore, biomechanical conditions such as tissue composition or perturbed physical conditions from a special geometry may play a key role in determining a dominant phenotype or inducing coexistence of both phenotypes. We already indicated the possible emergence of a third phenotype (Th17 for instance [41]) for intermediate doses of LPS in an earlier analysis in Figure 6. This conceptual framework does not conflict with the pivotal role of Th1- and Th2-associated cytokines in response to high- and low-dose LPS and may add another level of regulation.

Figure 14 shows the density profiles of Th1 and Th2 cells in $\alpha - D_L$ plane, where D_L is the diffusion coefficient of regulating factors (IFN-γ, IL-4, IL-12, TNF-α) and random motilities of cells (Th1 cells, Th2 cells, Th0 cells, macrophages)

on the left half plane of domain, $\Omega_1 = [0, 0.5] \times [0, 1]$. Various amounts of LPS ($\alpha = 0.1, 0.3, 1, 3, 10$) were assigned in each column. In each column, a range of diffusion coefficients (D_L^i= i-th row ($i = 1, \ldots, 5$); $D_L^1 < D_L^2 < D_L^3 < D_L^4 < D_L^5$) were used on the left half domain (Ω_1) while the fixed base values of diffusion coefficients were used on the right half domain $\Omega_2 = [0.5, 1] \times [0, 1]$. Dominant phenotypes were enclosed in the 'green' dotted line in Figures 14A-14B. As in the previous simulations in Figure 13, Th1 cells tend to become a dominant cell type as the LPS level (α) is increased overall. However, the corresponding LPS level for a switch from a Th2-dominant phase to a Th1-dominant phase differs according to diffusion coefficients D_L^i. For example, Th1 cells are already a dominant phenotype for the low LPS level ($\alpha = 1\mu g$) when smaller diffusion coefficients ($D_L^i, i = 1, 2, 3$) were used. A threshold α^{th} of the LPS levels for a switch from type II asthma to type I asthma was marked as a 'brown star' in the 3rd row. This threshold value α^{th} (brown star; $0.3 < \alpha^{th} < 1$) for an intermediate diffusion (D_L^3) moves to a higher value α_*^{th} ('yellow star' in the 4th row; $1 < \alpha_*^{th} < 3$). Therefore, faster diffusions in the relatively soft tissue may promote interactions between Th1 cells and macrophages, and suppress activities of Th2 cells and Th2-associated cytokines. In this case, Th1 cells become a dominant phenotype for relatively lower doses of LPS. This model prediction implies that stiffness in tissue in the microenvironment may play an important role in regulation of Th1/Th2 cell phenotypes in response to LPS level (α). Macrophages also follow similar patterns.

4. **Discussion.** Asthma is a common chronic inflammatory disorder of the airways associated with obstruction and hyperresponsiveness of airways [25, 13]. The microenvironment in asthma development includes various cell types such as T cells, eosinophils, mast cells, and neutrophils [41]. These cells are involved in the immune and inflammatory responses to allergens and communicate with one another and influence each others' behavior by means of the cytokines and growth factors they secrete. Among those cells, the development of memory T cells is a crucial step in the regulation of the inflammatory responses [104, 39]. A large number of studies support the notion that an imbalance between Th1 and Th2 cytokines, favoring the Th2 immune response (with a decrease in Th1 response), is the main cause of inflammation reactions in asthma development [41]. This so called Th2 hypothesis of asthma pathogenesis was first suggested by Mosmann in 1989 [78], based on earlier discovery of the presence of two distinct subtypes of Th cells in mice: Th1 and Th2 [77]. Inflammation induced by Th2 cytokines can promote the secretion of more inflammatory mediators including other chemokines and cytokines via positive feedback loops [41]. T cell-derived molecules for Th1 cells include IL-2, IFN-γ, and IL-12 while other molecules such as IL-4, -5, -9, -13, and -25 are associated with Th2 cells [41]. Recent studies found that Th-17-associated cytokines were also implicated in asthma immunobiology [41, 73]. Other cytokines include various growth factors (EGF, FGF, PDGF, TGF-β), anti-inflammatory cytokines (IL-10 and IL-18), proinflammatory cytokines (IL-1β, -6, and -11; TNF-α, GMCSF) that are involved in the innate host defense, and chemokines or chemotactic cytokines (IL-8, RANTES, eotaxin, MCP-1, MCP-5) [41].

LPS can be found in the air including particles [71, 35] and various doses of LPS are known to lead to the development of two distinct phenotypes, Th1 or Th2 [53]. Despite the evidence supporting Th2 hypothesis, studies in humans have found that

the levels of both Th1 and Th2 cytokines are elevated in the airways and blood of asthma patients [21, 67].

In this paper, we focused on identifying the basic 'flip-flop' dynamics of type I and type II asthma in response to various doses of LPS. We developed a mathematical model of the mutual antagonism between Th1 and Th2 phenotypes. The model considers densities of cells (Th1 cells, Th2 cells, Th0 cells, and macrophages) and concentrations of key regulatory molecules (IFN-γ, IL-4, IL-12, TNF-α). The simulation results from the model are in a good agreement with experimental data in [53]. The results are summarized as follows:

- Th2 cells become dominant for low LPS levels ($\alpha \leq 1$) while Th1 cells become a major phenotype for high LPS levels ($\alpha \geq 10$). For low doses of LPS ($\alpha = 1$), IL-4 levels are upregulated while the concentrations of IL-12 and IFN-γ are down-regulated. The high level of IL-4 induces the Th2 dominant system and suppresses the Th1 cell phenotype. On the other hand, populations of Th1 cells and macrophages become dominant for high levels of LPS ($\alpha \geq 10$) due to downregulation of IL-4 and elevated IL-12 and IFN-γ, which further suppress the Th2 cell proliferation.
- Steady states of two key phenotypes as a function of the injected LPS level (α) illustrate this switching behavior between Th1 and Th2 cells and also suggest coexistence of those two phenotypes in a narrow interval of intermediate levels of LPS ($2 < \alpha < 7$) (Figure 6). This might suggest emergence of the third dominating phenotype such as Th17 [41]. In light of the flexibility and applicability of the current model, further investigation of such a model is warranted, and the results of this analysis as well as experimental validation will be reported elsewhere in future.
- High (low) levels of IL-12 were associated with high (low) LPS levels in both experiments and model simulations (Figure 8).
- Macraphage numbers increased according to LPS levels, which is consistent with the experimental observation (Figure 9).
- The current model also predicts that the IL-4 level is significantly decreased when TNF-α-deficient mice are used compared to the wild type (Figure 10).
- We found that infiltration of macrophages is significantly decreased in response to high-doses LPS ($\alpha = 10, 100$) in IFN-γ-deficient (IFN-$\gamma^{-/-}$) mice, compared to the wild type (Figure 11). Simulation results also indicate that the knockdown of IL-4 in the case of the high doses of LPS ($\alpha = 10$) does not affect the macrophage population.
- Levels of IL-12, a Th2-associated cytokine, were also significantly reduced in IFN-$\gamma^{-/-}$ mice in response to high doses of LPS ($\alpha = 10, 100$; Figure 12).
- We also investigated the role of microenvironment in determining the dominant phenotype in asthma development. The model predicts that a perturbation of the microenvironment might lead to different types of asthma. The model also shows that faster diffusion processes may favor interactions between Th1 cells and macrophages, and suppress Th2 cells, leading to type I asthma for relatively low doses (α=1 μg) of LPS (Figure 14). Isolated islands of one phenotype for an intermediate level of LPS ($\alpha = 3$; Figure 13B) can be found under a certain initial distribution of involved cells. These results show that the microenvironment plays a crucial role in the regulation of type I and type II asthma in response to various LPS levels.

Eosinophils are known to play a pivotal role in asthmatic airway remodeling through MMP production at inflammatory sites in response to stimuli from TNF-α [94]. Hints of possible treatment in severe asthma using TNF-α antagonism have been reported [45] due to its pivotal role in the initiation and perpetuation of airway inflammation, increased mucous production, AHR and airway remodeling in asthma. TNF-α is also known to play a critical role in immune surveillance against tumour cells and protection against infections [45, 15]. The importance of TNF-α in the control of airway inflammation and improved asthma control led to trials of TNF-α antagonists using a number of TNF-α inhibitors: etanercept (a soluble fusion protein combining two p75 TNFRs with an Fc fragment of human immunoglobulin [Ig]G1), infliximab (a chimeric mouse/humanized monoclonal [m]Ab) and adalimumab (a fully human mAb) [45]. TNF-α can upregulate tenascin and MMPs, a landmark of severity of the disease and airway remodeling espeically in the presence of eosinophils and fibroblasts through activation of the transcription factor Ets-1 [76, 94]. Large amounts of tenascin and MMPs are found in the sub-epithelial basement membrane (SBM) and produced by myofibroblasts and fibroblasts in the vicinity of the SBM. In the same vein, TNF-α enhances tissue remodeling via EGFR-dependent stresses and repairs by inducing proliferation of sub-epithelial myofibroblasts [75, 76]. Heterogeneity in response to TNF-α inhibition has been blamed for poor clinical outcome. Therefore, identifying new markers may help us establish which subset of this heterogeneous disease may benefit from TNF-α antagonism.

The "hygiene hypothesis" states that the chance of getting allergic diseases is increased by a hygienic childhood environment [38], leading to insufficient stimulation of Th1 cells and dominance of Th2 cells after allergen exposure [111]. However, a number of studies have shown that type I diabetes and other autoimmune diseases are mediated by Th1 cells [105]. Therefore, an alternative hypothesis known as the "counter-regulation hypothesis" was suggested to explain this phenomenon. This states that all types of infection may prevent the development of allergic reactions by inducing another type of T cell [92, 81] called regulatory T cells (Tregs). These cells inhibit potentially harmful immune responses [89] and contribute to the maintenance of immune homeostasis [64]. The two major types of Treg populations are the thymic-derived $CD4^+Foxp3^+$ Treg cells and adaptive $CD4^+$ Treg cells ($CD4^+Foxp3^-$) [64]. Recent studies [3, 4] also indicate that the population of allergen-specific Tregs increases the effectiveness of immunotherapies. Gross *et al.* (2011) [38] recently developed a mathematical model of allergy and Th1-Th2-Treg interactions by extending the previous model proposed by Behn *et al.* (2001) [11]. These authors [38] found that the model was able to capture the key events in allergen-specific immunotherapy. The model also predicted that the decisive effect of immunotherapy (suppression of Th2 cells and increased Tregs) depends on administration of injections immediately before the maintenance phase [38]. Tregs are believed to play a crucial role in regulating allergic disease such as asthma via two key cytokines, TGF-β and IL-10 [87, 6]. (See recent review articles [89, 64, 87, 108] for the role of Tregs in more detail). However, in experiments by Eisenbarth *et al.* (2002) [29] and Kim *et al.* (2007) [53], LPS-depleted OVA did not induce an inflammatory response in the lung (T cell anergy) instead of immune tolerance via Tregs, while OVA plus the low- and high-dose LPS induced typical Th2 cell responses and strong Th1 inflammatory responses, respectively. Therefore, we did not consider the role of Tregs in our model system. We plan to explore the important role of Tregs in asthma in future work.

Cosmi *et al.* [24] recently described a new subset of human memory $CD4^+$ T cells that secrete both IL-4 and IL-17A. This new type of T cell population, known as Th17/Th2 lymphocytes, was more prevalent in patients with allergic asthma than in the healthy population [23]. Th17 cells are able to produce IL-4, IL-5, IL-9 and IL-13 as well as IL-17A, IL-8, and IL-22 [23]. IL-4-rich microenvironment may favor the switch of Th17 lymphocytes toward Th17/Th2 phenotype based on the observation that Th17 cells expressed IL-4R and were susceptible to IL-4 activity while no STAT3 or STAT4 phosphorylation was observed in Th2 cells in response to IL-23 [24, 8]. It is also possible that allergen-specific Th2 cells take the role of producing IL-17 in response to inflammatory cues [23]. For example, it was reported in mice that IL-1β, IL-6, and IL-21 up-regulate IRF4 and RORγ gene expression and induce IL-17 production in Th2 cells in vitro, suggesting there is plasticity in the phenotypic changes observed in response to inflammatory stimuli [103]. IL-6 (along with TGFβ) up-regulates IL-17 expression in T cells via a STAT3-RORγt pathway [113]. In a Th17 immunity study, Th2 and Th17 cells (Th2- and Th17-related cytokines) were dominant phenotypes (cytokines) in allergic asthmatics, and the ratio of Th17 cells to Th2 cells and concentrations of IL-17 and IL-22 were increased according to the severity of the disease [112]. Kim *et al.* [55] found that IL-6 production was enhanced by high levels of LPS in the atopic asthma mouse model, and that the Th17 cell response induced by high levels of LPS is abolished in IL-6 knockout mice. A recent study [63] demonstrated the plasticity of Th17 cells upon differentiation, showing that TGFβ is a critical component for sustained IL-17A and IL-17F production by Th17 cells and that, in the absence of TGFβ, IL-12 and IL-23 can induce Th17 cells to secrete IFN-γ, a key Th1-related cytokine, in a T-bet- and STAT4-dependent manner. These data indicate Th17 cells can regulate production of cytokines depending on the microenvironmental inflammatory milieu [6]. Our simulations predicted the existence of the third phenotype, Th17, in a narrow window of intermediate LPS levels even though we did not specifically include known Th17-related cytokines such as IL-1β, IL-6, IL-21, and IL-23 in our model system. IL-4, the inducer of Th2 cells, might have influenced the response to intermediate levels of LPS via the interplay between players in our complex network of Th1-Th2 regulation in this study, as IL-4 derives phenotypic change from Th17 to Th17/Th2 populations [24, 23]. Or, IFN-γ secretion by Th17 cells under certain conditions [63] may generate the possibility of the onset of Th17 phenotype in our computational model system. How emergence or behaviors of Th17 cells are precisely regulated in the immune system is not presently completely understood and is still under active investigation. We will address this issue in future work by taking into consideration key Th17-related cytokines in an extended model.

Our model can be used to suggest the effect of potential drugs that will control the Th1/Th2 cell type regulations in asthma. For example, by introducing a TNF-α inhibitor that reduces Th2 cell population, the Th1 population becomes the dominant cell type. The results of the present paper can serve as a starting point for more comprehensive modeling and experimentation. These should include the following: (a) Detailed intra- and inter-celluar dynamics involving the STAT4 gene and allergen-specific IgE production. For example, the asthma phenotypes induced by the low dose LPS were completely inhibited in TNF-α receptor-deficient mice, while the asthma phenotypes associated with the high dose LPS were abolished by the homozygous null mutation of the STAT4 gene [53]. Detailed analysis of these would be possible when detailed signal transduction pathways are modeled and

integrated into an extended model. (b) As a part of the inflammatory response, many cell types migrate toward regional lymph nodes (LN) in response to chemotactic signals. During this course of action, motility of those different cell types and diffusion processes, thus chemical reactions, of the related molecules depend on tissue conditions in the microenvironment. For instance, their diffusion coefficients or chemotactic sensitivities would be different in a given composition of the ECM. (c) Mechanical feedbacks from the stroma near the regional LN and mechanical stress near blood vessels in the events of asthmatic airway remodeling. (d) Recruitment of other stromal cells such as fibroblasts/myofibroblasts which are known to be associated with secretion of ECM-degrading molecules such as MMPs, thus leading to airway remodeling [41]. Fibroblasts play a significant role in promoting this proteolytic activity and loss of stability near the basal membrane. This type of strategy, using other cells in the microenvironment, has long been observed in angiogenesis, tumor growth [54], tumor invasion [50, 52], and wound healing.

We plan to build a multi-scale model that takes into account inter- and intracellular dynamics as well as interactions between inflammatory cells and stromal cells; some hybrid models have been developed in the context of tumor growth [54, 5]. But any model that will take into consideration these processes will involve the pathways of TNF-α, IFN-γ, IL-4, and IL-12 as key players for the inhibition/enhancement of type I and II asthma. In this sense, the present paper is a first step toward more comprehensive modeling of mutual antagonism between type I and type II asthma in the patient-specific microenvironment.

Appendix A. Parameter estimation. *Random motility/diffusion coefficients*

$D_{H_1}, D_{H_2}, D_{H_0}$ (Th1, Th2, Th0 cells): Random motility of a typical animal cell has been estimated to be 1.8×10^{-6} cm^2/h [17]. Stokes and Lauffenburger (1991) [96] estimated the motility of endothelial cells to be 2.52×10^{-5} cm^2/h. In glioma invasion, the value of 4.176×10^{-7}-8.316×10^{-6} cm^2/h was used in [27] and [43] while Kim *et al.* [51] estimated it to be 3.6×10^{-8} cm^2/h. Random motility of T and B cells was reported, 67 and 12 $\mu m^2/min$ ($= 7.2\times10^{-6}$ cm^2/h) respectively in intact lymph node [72]. We take D_{H_1}=D_{H_2}=D_{H_0}=7.2×10^{-7} cm^2/h.

D_M (Macrophages): Stickle *et al.* (1985) [95] estimated the random motility of macrophages using a one-dimensional diffusion equation and experiments. They found that the random motility coefficient depends on concentration of FNLLP concentration (bell-shaped curve) and was in a range of 1×10^{-9} cm^2/s (at $0M$ FNLLP) - 1×10^{-8} cm^2/s (at $10^{-9}M$ FNLLP). In a follow-up study, Glasgow *et al.* [37] also showed that the random motility of a single cell was in good agreement with that of population studies from stimulus of FNLLP $(10^{-11}$-$10^{-7})M$ but this value was different in the absence of stimulus. Also see the qualitatively similar results from [28]. We take D_M= 3.6×10^{-7} cm^2/h.

D_{I_1} (IL-4), D_{I_2} (IL-12): Coombs *et al.* [22] estimated a diffusion coefficient of IL-4, 1.0×10^{-6} cm^2/s (=3.6×10^{-3} cm^2/h) in the study of the delivery of effector molecules. In a study of IL-4 kinetics for Th1/Th2 regulation, Jansson *et al.* [47] took 1.0×10^{-7} cm^2/s (=3.6×10^{-4} cm^2/h) from [33]. We take D_{I_1}=1.0×10^{-4} cm^2/h. We also take D_{I_2}=1.0×10^{-4} cm^2/h.

D_F (IFN-γ): A diffusion coefficient of chick Interferon was 3.4×10^{-3} cm^2/h in [59]. On the other hand, the apparent diffusion coefficient of IFNα in the lipidic

Par	Description	Dimensional value	Refs
	Random motility/Diffusion coefficient		
D_{H_1}	Random motility of TH1 phenotype	7.2×10^{-7} cm^2/h	[72]
D_{H_2}	Random motility of TH2 phenotype	7.2×10^{-7} cm^2/h	[72]
D_{H_0}	Random motility of TH0 phenotype	7.2×10^{-7} cm^2/h	[72]
D_M	Random motility of macrophages	3.6×10^{-7} cm^2/h	[95, 37]
D_F	Diffusion coefficient of IFN-γ	1.0×10^{-4} cm^2/h	[44]
D_{I_1}	Diffusion coefficient of IL-4	1.0×10^{-4} cm^2/h	[47, 33]
D_{I_2}	Diffusion coefficient of IL-12	1.0×10^{-4} cm^2/h	TW
D_T	Diffusion coefficient of TNF-α	1.2×10^{-3} cm^2/h	[82]
	Production		
α	LPS injection amount	$(0.1\text{-}100)\times10^6$ pg	[53]
β	Source of Th0 cells	1.0×10^4 $cells/(cm^3.h)$	TW
λ_1	IFN-γ secretion rate by Th1 cells	1.68×10^{-2} h^{-1}	[53],TW
λ_2	Proliferation parameter of Th2 cells	7.14×10^{-10} $cm^6pg^{-2}h^{-1}$ (k=1)	[36, 40, 26, 46]
λ_3	IL-4 secretion rate by Th2 cells	1.0×10^{-7} h^{-1}	[53], TW
λ_4	TNF-α production rate by Th1	5.0×10^{-9} h^{-1}	[97, 53], TW
λ_5	Proliferation parameter of Th1 cells	2.6×10^{-10} $cm^3pg^{-1}h^{-1}$ (m=1)	[46, 36, 40, 26]
λ_8	IL-12 secretion rate by Th1 cells	8.8×10^{-6} h^{-1}	[53], TW
λ_{10}	IL-12 secretion ration by macrophages	8.8×10^{-7} h^{-1}	[53], TW
λ_{11}	TNF-α secretion rate by Th2 cells	4.0×10^{-8} h^{-1}	[97, 53], TW
λ_{12}	TNF-α secretion rate by macrophages	7.5×10^{-8} h^{-1}	[97, 53], TW
λ_{13}	IFN-γ -mediated production parameter of macrophages	4.6×10^{-13} $cm^3pg^{-1}h^{-1}$ (l=1)	[114, 53], TW
K_1	Carrying capacity of Th1 cells	$=12H_1^*$	[53], TW
K_2	Carrying capacity of Th2 cells	$=12H_2^*$	[53], TW
K_3	Carrying capacity of macrophages	$=10M^*$	[53], TW
	Inhibition parameters		
λ_6	Inhibition parameter of Th1	2.6×10^1 $pg.cm^{-3}$	TW
λ_7	Inhibition parameter of Th2	1.3×10^6 $pg.cm^{-3}$	TW
λ_9	Inhibition parameter of IL-12	2.4×10^6 pg	TW
λ_{14}	Inhibition parameter of macrophages	7.6×10^1 $pg.cm^{-3}$	TW

TABLE 1. Parameters that are used in the model. TW=this work.

matrix was estimated to be 5.8 (+/- 1.2) $\times10^{-8}$ cm^2/s (=$(1.66-2.52)\times10^{-4}$ cm^2/h) [44]. We take D_F=1.0×10^{-4} cm^2/h.

D_T (TNF-α): Narhi *et al.* [82] determined a diffusion coefficient of TNF-α , 3.3×10^{-7} cm^2/s (=1.2×10^{-3} cm^2/h), using the sedimentation velocity data for murine TNF-α in PBS. We take D_T= 1.2×10^{-3} cm^2/h.

Par	Description	Dimensional value	Refs
	Death/decay		
μ_{H_1}	Th1 cells	$1.0\times10^{-2}\ h^{-1}$	[106, 99, 90, 18, 57, 83]
μ_{H_2}	Th2 cells	$1.0\times10^{-2}\ h^{-1}$	[106, 99, 90, 18, 57, 83]
μ_{H_0}	Th0 cells	$1.0\times10^{-2}\ h^{-1}$	[106, 99, 90, 18, 57, 83]
μ_M	Macrophages	$0.2\ h^{-1}$	TW
μ_F	IFN-γ	$2.0\ h^{-1}$	[14], TW
μ_{I_1}	IL-4	$5.8\times10^{-2}\ h^{-1}$	[16, 80, 47]
μ_{I_2}	IL-12	$8\ h^{-1}$	TW
μ_T	TNF-α	$0.1\ h^{-1}$	[34],TW
	Chemotaxis		
χ	Chemotactic sensitivity of macrophages toward INF-γ	1.0008×10^{-10} $cm^5pg^{-1}h^{-1}$	[56, 50, 86, 96, 1], TW
λ_F	Chemotactic parameter	$\lambda_F = 1$	[56, 50]

TABLE 2. Parameters that are used in the model (continued from Table 1.

Var	Description	Dimensional Value	Refs.
τ	Time	$1\ h$	
L	Spatial reference length	$0.1\ cm$	
H_1^*	Density of Th1 cells	$1.0\times10^5\ cells/cm^3$	[53]
H_2^*	Density of Th2 cells	$1.0\times10^5\ cells/cm^3$	[53]
H_0^*	Density of Th0 cells	$1.0\times10^5\ cells/cm^3$	[53]
M^*	Density of macrophages	$5.0\times10^4\ cells/cm^3$	[107, 53]
F^*	Concentration of IFN-γ	$7.0\times10^5\ pg/cm^3$	[98]
I_1^*	Concentration of IL-4	$20\ pg/cm^3$	[53]
I_2^*	Concentration of IL-12	$40\ pg/cm^3$	[53]
T^*	Concentration of TNF-α	$250\ pg/cm^3$	[53]
α^*	LPS level	$1.0\times10^6\ pg$	[84, 53]

TABLE 3. Reference variables used in the model.

Chemotactic parameter (χ)

Chemotactic sensitivity can be in a range of (1.0×10^{-5}-2.0×10^{-1}) $cm^5g^{-1}s^{-1}$ [86, 96]. For example, the chemotactic sensitivity of myofibroblasts toward gradient of TGF-β can be (1.0×10^{-3}-1.0×10^{-2}) $cm^5g^{-1}s^{-1}$ [56, 50]. We take χ=2.8×10^{-2} $cm^5g^{-1}s^{-1}$.

Production rates

α (LPS level): We take α as a controlling parameter. To test the hypothesis on Th1/Th2 regulation in response to LPS levels as in [53], we take α= 0.1-100 μg.

λ_5 (proliferation rate of Th1 cells): Doubling times of Th1 and Th2 cells were estimated to be 6-24 h [36, 40, 26]. By using the reference value of Th0 cell density

(H_0^*) and a range of fraction values $\frac{I_2}{\lambda_6^m+I_1^m}$ = 0.1-1 (with $m = 1$) in the second term of equation (4), and a doubling time of τ=12 h from [46], we get a range of $\lambda_5 = \frac{\ln 2}{\tau f^\dagger}$=(57.7-577) $cm^3g^{-1}h^{-1}$ where $f^\dagger = \frac{I_2}{\lambda_6^m+I_1^m}H_0^*$. We take λ_5=2.6×10^2 $cm^3g^{-1}h^{-1}$.

λ_2 (proliferation rate of Th2 cells): By using the reference values of Th0 cells (H_0^*) and TNF-α (T^*=250 pg/cm^3), and a range of fraction values $\frac{I_1}{\lambda_7^k+F^k}$ = 0.001-1 (with $k = 1$) in the second term of equation (6), and a doubling time of $\tau = 12$ h [36, 40, 26, 46], we get a range of $\lambda_2 = \frac{\ln 2}{\tau f^\dagger}$ = (2.3×10^{12}-2.3×10^{15}) $cm^6g^{-2}h^{-1}$ where $f^\dagger = \frac{I_1}{\lambda_7^k+F^k}T^*H_0^*$. We take λ_2=7.14×10^{14} $cm^6g^{-2}h^{-1}$.

λ_1 (IFN-γ secretion rate by Th1 cells): IFN-γ levels are elevateded in a Th1-dominant phase. By using a range of Th1 cell density ($H_1^\dagger$=(1-10)H_1^*), 10-100 folds of IFN-γ basic levels (ΔF=(10-100)F^*), and $\frac{\Delta F}{\Delta t} = \lambda_1 H_1^\dagger$, we estimate λ_1 to be in a range of (1.7 × 10^{-3}-1.68×10^{-2}) h^{-1}. We take λ_1=1.68×10^{-2} h^{-1}.

λ_3 (IL-4 secretion rate by Th2 cells): In [53], IL-4 levels for wild type and $WT_{OVA} + LPS10$ were 20, 48 pg/ml, respectively. By using a range of Th2 cell density ($H_2^\dagger$=(0.01-1)H_2^*) and $\frac{\Delta I_1}{\Delta t} = \lambda_3 H_2^\dagger$, we estimate λ_3 to be in a range of (8.0×10^{-8}-8.0×10^{-6}) h^{-1}. We take λ_3=1.0×10^{-7} h^{-1}.

$\lambda_4, \lambda_{11}, \lambda_{12}$ (TNF-α secretion rates): In a study of rheumatoid arthritis [97], TNF-α levels were measured to be 3.0, 1.8, 4.2 pg/ml, respectively, after 12 hours for TTP-, TZF-, and mock-transduced Jurkat T cells with the initial concentration of 1.0×10^6 $cells/ml$. In Kim *et al.* [53], in the case of low doses of LPS, BAL TNF-α concentration went up to ∼260 pg/ml after 6 hours and saturated down to ∼20 pg/ml after 24 hours while the level of TNF-α increased upto ∼500 pg/ml and slowly saturated down to ∼400 pg/ml for high doses of LPS. From these observations, we take λ_4=5.0×10^{-9} h^{-1}, λ_{11}=4.0×10^{-8} h^{-1}, λ_{12}=7.5×10^{-8} h^{-1}.

λ_8, λ_{10} (IL-12 secretion rates): In the case of high doses of LPS, IL-12 levels were elevated to ∼800 pg/ml and ∼1100 pg/ml after 6 and 24 hours (OVA+LPS10) in [53]. On the other hand, low levels (∼(250-300) pg/ml) of IL-12 was observed for low levels of LPS. By using the reference value of Th1 cells (H_1^*), $\frac{\Delta I_2}{\Delta t} = \lambda_8 f^\dagger H_1^*$, λ_9=2.4 μg and a range of LPS levels ($0.1 < \alpha < 100$), where the fraction $f^\dagger = \frac{\alpha}{\lambda_9+\alpha} \sim \frac{\alpha}{2.4+\alpha}$=(0.04-0.9766), we get a range of estimated values λ_8=(4.6×10^{-7}-1.1×10^{-5}) h^{-1}. We take λ_8=8.8×10^{-6} h^{-1}. We also take λ_{10}= 8.8×10^{-7} h^{-1} in a similar fashion.

λ_{13} (IFN-γ -mediated production rate of macrophages): Doubling time (τ) of macrophages has been measured to be 35 h and 18-22 h for LPS treated cells and untreated cells, respectilvey [114]. Using a doubling time (τ=20 h) of macrophages, the reference value of Th1 cells (H_1^*), a range of relatively high levels of IFN-γ ($F^\dagger$=(1-10)F^*), and a range of IL-4 levels (I_1=(2-200) pg/cm^3), and fixing the inhibition parameter λ_{14}=76 pg/cm^3, we get a fraction of growth-assisting term $f^\dagger = \frac{F^\dagger}{\lambda_{14}^l+I_1^l}H_1^*$=(0.0253-0.897) g/cm^3 in the macrophage growth term in equation (13) (assuming l=1). So, we get a range of $\lambda_{13} = \frac{\ln 2}{\tau f^\dagger}$=3.86×10^{-2}-1.37. Taking into account high IFN-γ levels and low IL-4 levels in response to high LPS levels

(or, low IFN-γ levels and high IL-4 levels in response to low LPS levels), we take λ_{13}=4.6×10^{-1} $cm^3g^{-1}h^{-1}$.

Death/decay rate

$\mu_{H_1}, \mu_{H_2}, \mu_{H_0}$ (Th-cells): The half life of naive T cells in the absence of MHC molecules has been measured to be 3-4 weeks [106, 99, 90, 18, 57, 83]. From this, we get (1.0-1.4)×10^{-3} h^{-1}.

μ_{I_1} (IL-4): Nebulized IL-4R has a serum half-life of approximately 1 wk (∼0.0041 h^{-1}) [16] while pharmacokinetic analysis showed a prolonged half life of ∼ 5 days [80]. Jansson *et al.* estimated a decay rate of IL-4 (=1.152×10^{-1} h^{-1}) in a study of the regulation of Th1/Th2 cells [47]. We take a bit larger value, μ_{I_1}=5.8×10^{-2} h^{-1}.

μ_{I_2} (IL-12): A decay rate of IL-2 was 0.4167 h^{-1} (10 day^{-1}) in [58]. We take a relatively larger value μ_{I_2}=8.0 h^{-1}.

μ_F: The half life of IFN-γ is known to be 3.5-7.5 h in [14]. *In vivo*, IFN-γ is eliminated from the bloodstream with a half-life of 1.1 min, due to binding to heparan sulfate but unbound IFN-γ is cleaved rapidly with a half life of 99 min [65]. This leads to the decay rates of (37.8-0.42) h^{-1}. We take an intermediate value, μ_F=2.0h^{-1}.

μ_T: While the half life of TNF-α was estimated to be 18.2 min in [85], larger values of the half life (1-3 h) of TNF-α were reported in a study of TNF-α secretion by macrophages in response to LPS [34]. We take 6 hours of the half life, leading to μ_F=0.1 h^{-1}.

Appendix B. **Nondimensionalization.** We nondimensionalize the system of partial differential equations (21) in Mathematical model Section using variables introduced in the following:

$$
\begin{aligned}
&\bar{t} = \frac{t}{\tau},\ \bar{D}_{H_1} = \frac{D_{H_1}}{D},\ \bar{D}_{H_2} = \frac{D_{H_2}}{D},\ \bar{D}_{H_0} = \frac{D_{H_0}}{D},\ \bar{D}_M = \frac{D_M}{D},\\
&\bar{D}_F = \frac{D_F}{D},\ \bar{D}_{I_1} = \frac{D_{I_1}}{D},\ \bar{D}_{I_2} = \frac{D_{I_2}}{D},\ \bar{D}_T = \frac{D_T}{D},\ \bar{H}_1 = \frac{H_1}{H_1^*},\\
&\bar{H}_2 = \frac{H_2}{H_2^*},\ \bar{H}_0 = \frac{H_2}{H_0^*}, \bar{M} = \frac{M}{M^*},\ \bar{F} = \frac{F}{F^*},\ \bar{I}_1 = \frac{I_1}{I_1^*},\ \bar{I}_2 = \frac{I_2}{I_2^*},\ \bar{T} = \frac{T}{T^*},\\
&\bar{K}_1 = \frac{K_1}{H_1^*},\ \bar{K}_2 = \frac{K_2}{H_2^*},\ \bar{K}_2 = \frac{K_3}{M^*},\ \bar{\lambda}_1 = \frac{\lambda_1 \tau H_1^*}{F^*},\ \bar{\lambda}_2 = \frac{\lambda_2 \tau H_0^* T^* I_1^*}{(F^*)^k},\\
&\bar{\lambda}_3 = \frac{\lambda_3 \tau H_2^*}{I_1^*},\ \bar{\lambda}_4 = \frac{\lambda_4 \tau H_1^*}{T^*},\ \bar{\lambda}_5 = \frac{\lambda_5 \tau H_0^* I_2^*}{(I_1^*)^m},\ \bar{\lambda}_6 = \frac{\lambda_6}{I_1^*},\ \bar{\lambda}_7 = \frac{\lambda_7}{F^*},\\
&\bar{\lambda}_8 = \frac{\lambda_8 \tau H_1^*}{I_2^*},\ \bar{\lambda}_9 = \frac{\lambda_9}{\alpha^*},\ \bar{\lambda}_{10} = \frac{\lambda_{10} \tau M^*}{I_2^*},\ \bar{\lambda}_{11} = \frac{\lambda_{11} \tau H_2^*}{T^*},\\
&\bar{\lambda}_{12} = \frac{\lambda_{12} \tau M^*}{T^*},\ \bar{\lambda}_{13} = \frac{\lambda_{13} \tau F^* H_1^*}{(I_1^*)^l},\ \bar{\lambda}_{14} = \frac{\lambda_{14}}{I_1^*},\ \bar{\alpha} = \frac{\alpha}{\alpha^*},\ \bar{\beta} = \frac{\beta}{\beta^*},\\
&\bar{\chi} = \frac{\chi F^* \tau}{L^2},\ \bar{\mu}_{H_1} = \tau \mu_{H_1},\ \bar{\mu}_{H_2} = \tau \mu_{H_2},\ \bar{\mu}_{H_0} = \tau \mu_{H_0},\ \bar{\mu}_M = \tau \mu_M,\\
&\bar{\mu}_F = \tau \mu_F,\ \bar{\mu}_{I_1} = \tau \mu_{I_1},\ \bar{\mu}_{I_2} = \tau \mu_{I_2},\ \bar{\mu}_T = \tau \mu_T.
\end{aligned}
\tag{27}
$$

If we drop the bar("-") in the new variables and parameters, then the differential equations and boundary conditions remain unchanged. Reference values for main variables are listed in Table 3 and estimates of those values are described below:

M^* (Macrophages): OVA sensitization increased the number of macrophages from 5.0×10^4 $cells/cm^3$ to 13×10^4 $cells/cm^3$ compared to saline sensitization [107]. We take M^*=5.0×10^4 $cells/cm^3$.

F^* (IFN-γ): IFN-γ levels in OVA sensitization were increased in almost 6-fold compared to saline sensitization [107].

I_1^* (IL-4): From BAL IL-4 levels in [53], we use I_1^*=20 pg/cm^3.

I_2^* (IL-12): BAL IL-12p40 expression levels for OVA+LPS0.1 in [53] were 30 pg/cm^3 6 hours after allergen sensitization. We take I_2^*=40 pg/cm^3.

T^* (TNF-α): BAL TNF-α level for OVA+LPS0.1 in [53] was about 250 pg/cm^3 6 hours after allergen sensitization.

α^*: We take α as a controlling parameter. In [53], various amounts of LPS (α=0.1-100 μg) were injected in order to test the hypothesis on Th1/Th2 regulation. We take α^*=1.0 μg.

Appendix C. **Sensitivity analysis.** In the model developed in this paper there are some parameters for which no experimental data are known or that may affect significantly the simulation results. In order to determine the sensitivity of the cell populations (Th1 cells, Th2 cells, Th0 cells, and macrophages) and concentrations of regulating factors (IFN-γ, IL-4, IL-12, and TNF-α) to these parameters, we have performed sensitivity analysis for the model. We have chosen a range for each of these parameters and divided each range into 6000 intervals of uniform length. The base values of the parameters are as in Tables 1,2. For each of the parameters a partial rank correlation coefficient (PRCC) value is calculated. PRCC values range between -1 and 1 with the sign determining whether an increase in the parameter value will decrease (-) or increase (+) the cell populations and concentrations of involved regulating chemicals at a given time. Tables 4-6 summarize the results of the sensitivity analysis in terms of the populations of Th1 cells (H_1), Th2 cells (H_2), Th0 cells, and macrophages (M), and concentrations of IFN-γ (F), IL-4 (I_1), IL-12 (I_2), and TNF-α (T) at $t = 150, 300, 500$ h.

Figure 15 illustrates sensitivity analysis of all variables for the twenty seven parameters ($\lambda_i (i = 1, \ldots, 14)$, μ_{H1}, μ_{H2}, μ_{H0}, μ_M, μ_F, μ_{I1}, μ_{I2}, μ_T, K_1, K_2, K_3, α, β) at the final time ($t = 500$). For example, we show the sensitivity of Th1/Th2 phenotypes in response to the changes of parameter values in Figure 15A. One can see that growth behaviors of both Th1 and Th2 phenotypes are sensitive to the parameters $\lambda_3, K_1, K_2, \alpha$ among other parameters. In particular, the populations of these key phenotypes (H_1, H_2) are very sensitive to the changes in LPS levels (α) as predicted from model analysis in Figures 4-6, *i.e.,* strong positive (negative) correlations of the Th1 cells (Th2 cells) with the LPS injection amount (α). One can also observe that the populations and concentrations of most of other variables (Th0 cells, macrophages, IFN-γ , IL-4, IL-12) are also very sensitive to the LPS input level (α) (see H_0, M, F, I_1, I_2 in Figures 15B, 15C, 15D). It is also natural to predict the positive correlation of the populations of Th1 and Th2 cells with their carrying capacities K_1 and K_2, respectively. The IFN-γ concentration (F) is positively correlated with the parameters $\lambda_1, \mu_{I_1}, K_1, \alpha$ but is negatively

Par PRCC	λ_1	λ_2	λ_3	λ_4	λ_5	λ_6	λ_{13}
$H_1(150)$	0.1760*	-0.216*	-0.441*	-0.0179	0.2493*	-0.0064	0.0146
$H_2(150)$	-0.134*	0.1932*	0.3614*	0.0149	-0.186*	0.0217	0.0078
$H_0(150)$	0.1133*	-0.193*	-0.0301	-0.042*	-0.134*	0.0051	-0.035*
$M(150)$	0.3037*	-0.161*	-0.472*	-0.0264	0.2036*	0.0037	0.1648*
$F(150)$	0.6820*	-0.208*	-0.422*	-0.0200	0.2440*	-0.0072	0.0218
$I_1(150)$	-0.147*	0.2032*	0.7482*	0.0265	-0.196*	0.0075	0.0024
$I_2(150)$	0.1423*	-0.118*	-0.283*	-0.0038	0.1209*	0.0123	0.0737*
$T(150)$	0.0965*	0.0262	-0.078*	0.0800*	0.0127	0.0083	0.0901*
$H_1(500)$	0.1578*	-0.201*	-0.403*	-0.0126	0.2170*	-0.0101	0.0049
$H_2(500)$	-0.121*	0.1701*	0.3158*	0.0167	-0.157*	0.0183	0.0050
$H_0(500)$	-0.035*	-0.068*	0.0428*	-0.0201	-0.148*	0.0371*	-0.0138
$M(500)$	0.1478*	-0.153*	-0.356*	-0.0122	0.1680*	0.0021	0.0278
$F(500)$	0.4538*	-0.201*	-0.390*	-0.0137	0.2184*	-0.0115	0.0119
$I_1(500)$	-0.125*	0.1742*	0.6448*	0.0294	-0.159*	0.0025	-0.0044
$I_2(500)$	0.1347*	-0.174*	-0.352*	-0.0083	0.1811*	-0.0028	0.0138
$T(500)$	0.0086	0.0160	-0.0322	0.0620*	0.0111	0.0009	0.0069
Min	1.2	0.00026	0.25	0.001	0.026	0.65	0.8
Base	2.4	0.00051	0.5	0.002	0.052	1.3	1.6
Max	3.6	0.00077	0.75	0.003	0.078	2	2.4

TABLE 4. Sensitivity analysis for the local ODE system. Parameters used in sensitivity analysis and PRCC values of Th1 cell type (H_1), Th2 cell type (H_2), Th0 cell type (H_0), macrophages (M), IFN-γ (F), IL-4 (I_1), IL-12 (I_2), TNF-α (T) at various time points ($t = 150, 300, 500$) are twenty seven perturbed parameters ($\lambda_i (i = 1, \ldots, 14), \mu_{H1}, \mu_{H2}, \mu_{H0}, \mu_M, \mu_F, \mu_{I1}, \mu_{I2}, \mu_T, K_1, K_2, K_3, \alpha, \beta$) here and Tables 5,6. A range (minimum/maximum) of these perturbed (non-dimensional) parameters and their baseline are given in the lower section. Sample size=6000. *Significant (p-value < 0.01).

correlated with $\lambda_3, \mu_{H_1}, \mu_F, K_2$. Similar analyses were performed on all other variables (H_0, M, F, I_1, I_2, T). For instance, we found that populations of Th1 cells and macrophages, and concentrations of IFN-γ and IL-12 (Th2 cells, Th0 cells, IL-4) are negatively (positively) correlated with IL-4 secretion rate (λ_3). However, the parameter (λ_3) has little correlation with TNF-α. For more details, see Tables 4-6.

The sensitivity analysis described above was carried out using the method from [68] and Matlab files available from the website of Denise Kirschner's Lab: http://malthus.micro.med.umich.edu/lab/usadata/.

Abbreviations. *AHR* = Airway hyperresponsiveness
APCs = Antigen-presenting cells
BAL = Bronchoalveolar lavage
DRS = Dose-response curve
ECM = Extracellular Matrix
EGF = Epidermal Growth Factor

Par	λ_7	λ_8	λ_9	λ_{10}	λ_{11}	λ_{12}	μ_2
$H_1(150)$	0.0251	0.0744*	-0.113*	0.1393*	-0.098*	-0.122*	0.1254*
$H_2(150)$	-0.0119	-0.123*	0.0707*	-0.046*	0.0769*	0.1237*	-0.397*
$H_0(150)$	0.0689*	-0.138*	0.0489*	-0.0139	-0.159*	-0.0082	-0.050*
$M(150)$	0.0124	0.0870*	-0.071*	0.1072*	-0.089*	-0.088*	0.1265*
$F(150)$	0.0153	0.0788*	-0.100*	0.1284*	-0.099*	-0.122*	0.1098*
$I_1(150)$	-0.0117	-0.135*	0.0727*	-0.039*	0.0881*	0.1399*	-0.378*
$I_2(150)$	0.0000	0.3046*	-0.201*	0.1476*	-0.051*	-0.066*	0.0628*
$T(150)$	0.0168	-0.034*	-0.0012	0.0275	0.5044*	0.4276*	-0.187*
$H_1(500)$	0.0221	0.0796*	-0.098*	0.1026*	-0.101*	-0.110*	0.1262*
$H_2(500)$	-0.0076	-0.103*	0.0506*	-0.0310	0.0595*	0.1124*	-0.422*
$H_0(500)$	0.1179*	-0.119*	0.0461*	-0.0289	-0.124*	0.0826*	-0.173*
$M(500)$	0.0142	0.0798*	-0.060*	0.0850*	-0.080*	-0.080*	0.1097*
$F(500)$	0.0126	0.0858*	-0.091*	0.0935*	-0.097*	-0.110*	0.1140*
$I_1(500)$	-0.0070	-0.113*	0.0533*	-0.0172	0.0707*	0.1251*	-0.401*
$I_2(500)$	0.0137	0.2929*	-0.212*	0.1028*	-0.095*	-0.077*	0.1008*
$T(500)$	0.0159	-0.0258	-0.0125	0.0326	0.4666*	0.3345*	-0.149*
Minn	0.95	11	1.2	0.55	0.008	0.0075	0.005
Base	1.9	22	2.4	1.1	0.016	0.015	0.01
Max	2.8	33	3.6	1.7	0.024	0.022	0.015

Par PRCC	μ_5	μ_6	μ_7	μ_8	K_1	K_2	K_3
$H_1(150)$	-0.202*	0.3215*	-0.248*	0.1809*	0.7114*	-0.347*	0.0563*
$H_2(150)$	0.1697*	-0.289*	0.1710*	-0.175*	-0.349*	0.6564*	0.0637*
$H_0(150)$	-0.095*	0.0230	0.1179*	0.2002*	-0.238*	-0.427*	-0.035*
$M(150)$	-0.293*	0.4018*	-0.199*	0.1406*	0.4055*	-0.386*	0.6227*
$F(150)$	-0.697*	0.3147*	-0.236*	0.1716*	0.6330*	-0.336*	0.0456*
$I_1(150)$	0.1731*	-0.730*	0.1705*	-0.181*	-0.359*	0.5709*	0.0746*
$I_2(150)$	-0.162*	0.2138*	-0.458*	0.0885*	0.3962*	-0.229*	0.1305*
$T(150)$	-0.052*	0.0957*	-0.0303	-0.766*	0.0839*	0.2867*	0.4501*
$H_1(500)$	-0.185*	0.3346*	-0.208*	0.1793*	0.5890*	-0.410*	0.0202
$H_2(500)$	0.1408*	-0.260*	0.1444*	-0.155*	-0.317*	0.6577*	0.0534*
$H_0(500)$	0.0438*	-0.0157	0.1216*	0.0806*	-0.296*	-0.362*	0.0299
$M(500)$	-0.174*	0.3088*	-0.164*	0.1428*	0.2748*	-0.367*	0.3276*
$F(500)$	-0.483*	0.3327*	-0.202*	0.1752*	0.4825*	-0.408*	0.0144
$I_1(500)$	0.1412*	-0.640*	0.1374*	-0.154*	-0.323*	0.5197*	0.0660*
$I_2(500)$	-0.163*	0.2940*	-0.418*	0.1542*	0.3999*	-0.377*	0.0503*
$T(500)$	-0.0039	0.0716*	-0.043*	-0.685*	0.0228	0.2674*	0.3376*
Min	1	0.029	4	0.05	6	6	5
Base	2	0.058	8	0.1	12	12	10
Max	3	0.087	12	0.15	18	18	15

TABLE 5. Sensitivity analysis (continued from Table 4)

FEV1 = Forced Expiratory Volume at 1 s
FGF = Fibroblast Growth Factor
GMCSF = Granulocyte/Macrophage Colony Stimulating Factor

Par PRCC	λ_{14}	μ_1	μ_3	μ_4	α	β
$H_1(150)$	-0.0169	-0.453*	0.0007	-0.0147	0.7694*	0.1722*
$H_2(150)$	0.0278	0.0400*	-0.0215	-0.0085	-0.664*	0.2102*
$H_0(150)$	0.0003	-0.052*	-0.0111	0.0213	-0.556*	0.2673*
$M(150)$	-0.0166	-0.312*	-0.0114	-0.208*	0.6426*	0.0446*
$F(150)$	-0.0133	-0.424*	0.0040	-0.0197	0.7430*	0.1465*
$I_1(150)$	0.0286	0.0426*	-0.0187	-0.0167	-0.670*	0.1870*
$I_2(150)$	-0.0214	-0.255*	-0.0013	-0.074*	0.9190*	0.0627*
$T(150)$	0.0114	-0.176*	-0.0182	-0.123*	-0.039*	0.1629*
$H_1(500)$	-0.0095	-0.517*	0.0032	-0.0154	0.7329*	0.1113*
$H_2(500)$	0.0275	0.0288	-0.0191	-0.0015	-0.599*	0.2010*
$H_0(500)$	0.0058	-0.065*	-0.0079	-0.0031	-0.579*	0.2372*
$M(500)$	-0.0079	-0.194*	0.0022	-0.067*	0.5903*	0.0250
$F(500)$	-0.0078	-0.498*	0.0056	-0.0197	0.7164*	0.0835*
$I_1(500)$	0.0277	0.0296	-0.0135	-0.0161	-0.590*	0.1624*
$I_2(500)$	-0.0046	-0.381*	0.0063	-0.0098	0.9092*	0.0627*
$T(500)$	0.0172	-0.126*	-0.0199	-0.038*	0.0087	0.1611*
Min	1.9	0.005	0.005	0.1	0.01	0.5
Base	3.8	0.01	0.01	0.2	10	1
Max	5.7	0.015	0.015	0.3	1e+002	1.5

TABLE 6. Sensitivity analysis (continued from Table 5)

IFN-γ = Interferon-γ
IFNα = Interferon-α
IL-4 = Interleukin-4
IL-12 = Interleukin-12
IP-10 = IFN-γ-inducible protein 10
LPS = Lipopolysaccharide
MCP = Monocyte Chemoattractant Protein
MMP = Matrix Metalloproteinase
Penh = enhanced pause
PDGF = Plateletderived Growth Factor
PFT = Pulmonary Function Test
STAT = Signal Transducer and Activator of Transcription
TGF-β = Transforming Growth Factors-β
Th1 = T helper type 1
Th2 = T helper type 2
TNF-α = Tumour Necrosis Factor-α
TNFR = Tumour Necrosis Factor Receptor
WT = Wild Type

REFERENCES

[1] R. Abe, S. Donnelly, T. Peng, R. Bucala and C. Metz, *Peripheral blood fibrocytes: differentiation pathway and migration to wound sites*, J. Immunol., **166** (2001), 7556–7562.

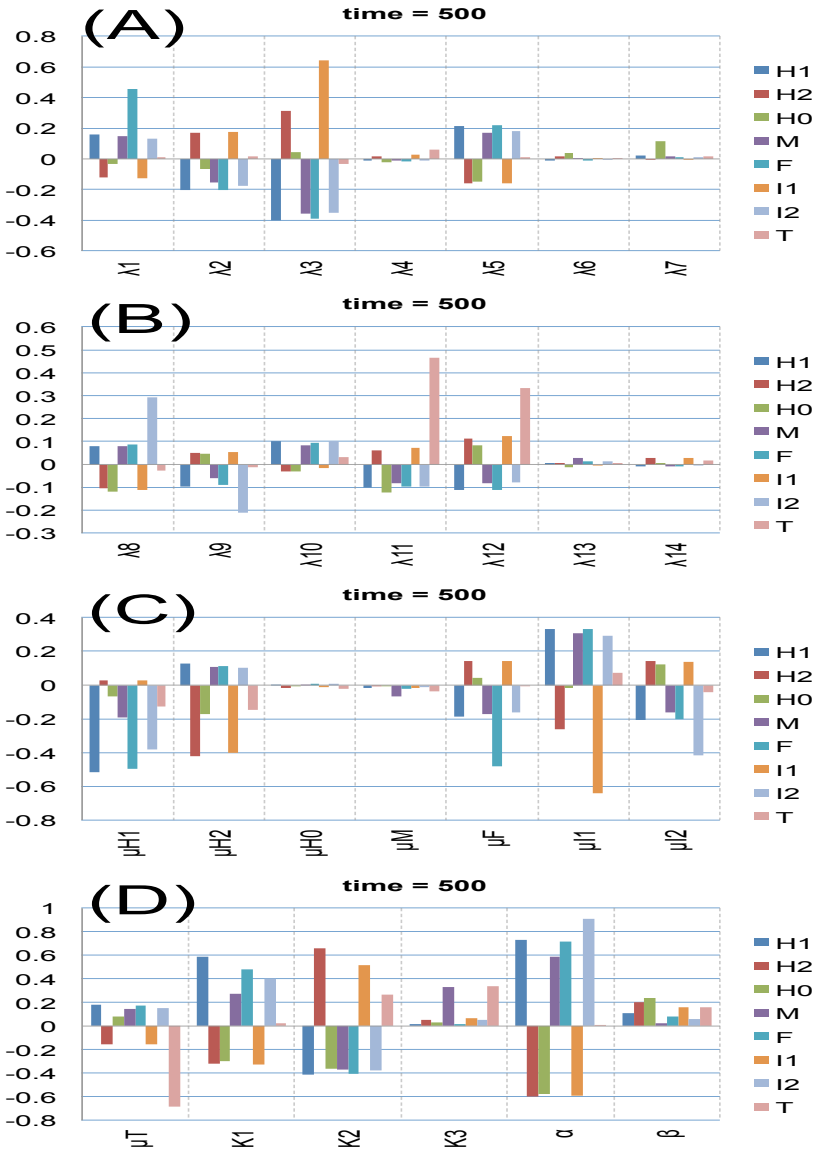

FIGURE 15. Sensitivity Analysis of the model. General Latin Hypercube Sampling (LHS) scheme and Partial Rank Correlation Coefficient (PRCC) performed on the model. The reference outputs are the densities and concentrations of main variables at the final time (t=500). The y-values in panels (A-D) indicate PRCC values of all variables $(H_1, H_2, H_0, M, F, I_1, I_2, T)$ for model parameters λ_i (i=1,...,7) in (A), λ_i (i=7,...,14) in (B), $\mu_{H_1}, \mu H_2, \mu H_0, \mu_M, \mu_F, \mu_{I_1}, \mu I_2$ in (C), $\mu_T, K_1, K_2, K_3, \alpha, \beta$ in (D), respectively. The analysis was carried out using the method of [68] with sample size 6000.

[2] O. Akbari, G. Freeman, E. Meyer, E. Greenfield, T. Chang, A. Sharpe, G. Berry, R. DeKruyff and D. Umetsu, *Antigen-specific regulatory T cells develop via the ICOS-ICOS-ligand pathway and inhibit allergen-induced airway hyperreactivity,* Nat. Med., **8** (2002), 1024–1032.
[3] C. A. Akdis, T. Blesken, M. Akdis, B. Wüthrich and K. Blaser, *Role of interleukin 10 in specific immunotherapy,* J. Clin. Invest., **102** (1998), 98–106.
[4] M. Akdis and C. A. Akdis, *Mechanisms of allergen-specific immunotherapy,* J. Allergy Clin. Immunol., **119** (2007), 780–791.
[5] T. Alarcón, H. Byrne and P. Maini, *Towards whole-organ modelling of tumour growth,* Prog. Biophys. Mol. Biol., **85** (2004), 451–472.
[6] J. F. Alcorn, C. R. Crowe and J. K. Kolls, *T_H17 cells in asthma and COPD,* Annu. Rev. Physiol., **72** (2010), 495–516.
[7] D. Amsen, A. Antov, D. Jankovic, A. Sher, F. Radtke, A. Souabni, M. Busslinger, B. McCright, T. Gridley and R. Flavell, *Direct regulation of Gata3 expression determines the T helper differentiation potential of Notch,* Immunity, **27** (2007), 89–99.
[8] F. Annunziato, L. Cosmi and S. Romagnani, *Human and murine Th17*, Curr. Opin. HIV AIDS, **5** (2010), 114–119.
[9] P. Barnes, *Th2 cytokines and asthma: An introduction,* Respir. Res., **2** (2001), 64–65.
[10] R. L. Baror and L. Segel, *On the role of a possible dialogue between cytokine and TCR-presentation mechanisms in the regulation of autoimmune disease*, J. Theor. Biol., **190** (1998), 161–178.
[11] U. Behn, H. Dambeck and G. Metzner, *Modeling Th1-Th2 regulation, allergy, and hyposensitization,* in "Dynamical Modeling In Biotechnology," Lectures Presented at the EU Advanced Workshop, Universität Leipzig NTZ 48/1997, World Scientific, Singapore, (2000), 227–243.
[12] M. Berry, C. Brightling, I. Pavord and A. Wardlaw, *TNF-alpha in asthma*, Curr. Opin. Pharmacol., **7** (2007), 279–282.
[13] B. Bochner, B. Undem and L. Lichtenstein, *Immunological aspects of allergic asthma,* Annu. Rev. Immunol., **12** (1994), 295–335.
[14] A. Bolinger and M. Taeubel, *Recombinant interferon gamma for treatment of chronic granulomatous disease and other disorders,* Clin. Pharm., **11** (1992), 834–850.
[15] T. Bongartz, A. Sutton, M. Sweeting, I. Buchan, E. Matteson and V. Montori, *Anti-TNF antibody therapy in rheumatoid arthritis and the risk of serious infections and malignancies: Systematic review and meta-analysis of rare harmful effects in randomized controlled trials,* JAMA, **295** (2006), 2275–2285.
[16] L. Borish, H. Nelson, M. Lanz, L. Claussen, J. Whitmore, J. Agosti and L. Garrison, *Interleukin-4 receptor in moderate atopic asthma. A phase I/II randomized, placebo-controlled trial,* Am. J. Respir. Crit. Care Med., **160** (1999), 1816–1823.
[17] D. Bray, "Cell Movements: From Molecules to Motility," Garland Pub., 2000.
[18] T. Brocker, *Survival of mature CD4 T lymphocytes is dependent on major histocompatibility complex class II-expressing dendritic cells,* J. Exp. Med., **186** (1997), 1223–1232.
[19] R. Callard and A. Yates, *Immunology and mathematics: Crossing the divide*, Immunology, **115** (2005), 21–33.
[20] J. Carneiro, J. Stewart, A. Coutinho and G. Coutinho, *The ontogeny of class-regulation of CD4+T lymphocte populations,* Int. Immunol., **7** (1995), 1265–1277.
[21] S. Cho, L. Stanciu, S. Holgate and S. Johnston, *Increased interleukin-4, interleukin-5, and interferon-gamma in airway CD4+ and CD8+ T cells in atopic asthma,* Am. J. Respir. Crit. Care Med., **171** (2005), 224–230.
[22] D. Coombs and B. Goldstein, *Effects of the geometry of the immunological synapse on the delivery of effector molecules*, Biophys. J., **87** (2004), 2215–2220.
[23] L. Cosmi, F. Liotta, E. Maggi, S. Romagnani and F. Annunziato, *Th17 cells: New players in asthma pathogenesis,* Allergy, **66** (2011), 989–998.
[24] L. Cosmi, L. Maggi, V. Santarlasci, M. Capone, E. Cardilicchia and F. F. et al., *Identification of a novel subset of human circulating memory CD4(+) T cells that produce both IL-17A and IL-4*, J. Allergy Clin. Immunol., **125** (2010), 222–230.
[25] E. Cutz, H. Levison and D. Cooper, *Ultrastructure of airways in children with asthma,* Histopathology, **2** (1978), 407–421.
[26] E. Deenick, A. Gett and P. Hodgkin, *Stochastic model of T cell proliferation: A calculus revealing IL-2 regulation of precursor frequencies, cell cycle time, and survival,* J. Immunol., **170** (2003), 4963–4972.

[27] T. Demuth, N. Hopf, O. Kempski, D. Sauner, M. Herr, A. Giese and A. Perneczky, *Migratory activity of human glioma cell lines in vitro assessed by continuous single cell observation*, Clin. Exp. Metastasis, **18** (2000), 589–597.
[28] T. V. Dyke, A. Reilly and R. Genco, *Regression line analysis of neutrophil chemotaxis,* Immunopharmacology, **4** (1982), 23–39.
[29] S. Eisenbarth, D. Piggott, J. Huleatt, I. Visintin, C. Herrick and K. Bottomly, *Lipopolysaccharide-enhanced, toll-like receptor 4-dependent T helper cell type 2 responses to inhaled antigen,* J. Exp. Med., **196** (2002), 1645–1651.
[30] M. Fishman and A. Perelson, *Modeling T cell-antigen presenting cell interactions,* J. Theor. Biol., **160** (1993), 311–342.
[31] M. Fishman and A. Perelson, *Th1/2 cross-regulation,* J. Theor. Biol., **170** (1994), 25–56.
[32] M. Fishman and A. Perelson, *Th1/Th2 differentiation and cross regulation,* Bull. Math. Biol., **61** (1999), 403–436.
[33] K. Francis and B. Palsson, *Effective intercellular communication distances are determined by the relative time constants for cyto/chemokine secretion and diffusion,* Proc. Natl. Acad. Sci. USA, **94** (1997), 12258–12262.
[34] J. Gao, Q. Xue, C. Papasian and D. Morrison, *Bacterial DNA and lipopolysaccharide induce synergistic production of TNF-alpha through a post-transcriptional mechanism,* J. Immunol., **166** (2001), 6855–6860.
[35] J. Gereda, D. Leung, A. Thatayatikom, J. Streib, M. Price, M. Klinnert and A. Liu, *Relation between house-dust endotoxin exposure, type 1 T-cell development, and allergen sensitisation in infants at high risk of asthma*, Lancet., **355** (2000), 1680–1683.
[36] A. Gett and P. Hodgkin, *A cellular calculus for signal integration by T cells,* Nat. Immunol., **1** (2000), 239–244.
[37] J. Glasgow, B. Farrell, E. Fisher, D. Lauffenburger and R. Daniele, *The motile response of alveolar macrophages. an experimental study using single-cell and cell population approaches,* Am. Rev. Respir. Dis., **139** (1989), 320–329.
[38] F. Groß, G. Metznerb and U. Behn, *Mathematical modelling of allergy and specific immunotherapy: Th1-Th2-Treg interactions,* J. Theor. Biol., **269** (2011), 70–78.
[39] G. Grunig, M. Warnock, A. Wakil, R. Venkayya, F. Brombacher, D. Rennick, D. Sheppard, M. Mohrs, D. Donaldson, R. Locksley and D. Corry, *Requirement for IL-13 independently of IL-4 in experimental asthma,* Science, **282** (1998), 2261–2263.
[40] H. Gudmundsdottir, A. Wells and L. Turka, *Dynamics and requirements of T cell clonal expansion in vivo at the single-cell level: effector function is linked to proliferative capacity,* J. Immunol., **162** (1999), 5212–5223.
[41] Q. Hamid and M. Tulic, *Immunobiology of asthma*, Annu. Rev. Physiol., **71** (2009), 489–507.
[42] M. Harber, A. Sundstedt and D. Wraith, *The role of cytokines in immunological tolerance: potential for therapy,* Expert. Rev. Mol. Med., **2** (2000), 1–20.
[43] B. Hegedus, J. Zach, A. Czirok, J. Lovey and T. Vicsek, *Irradiation and taxol treatment result in non-monotonous, dose-dependent changes in the motility of glioblastoma cells,* J. Neurooncol., **67** (2004), 147–157.
[44] S. Herrmann, G. Winter, S. Mohl, F. Siepmann and J. Siepmann, *Mechanisms controlling protein release from lipidic implants: Effects of peg addition,* Journal of Controlled Release, **118** (2007), 161–168.
[45] P. Howarth, K. Babu, H. Arshad, L. Lau, M. Buckley, W. McConnell, P. Beckett, M. Ali, A. Chauhan, S. Wilson, A. Reynolds, D. Davies and S. Holgate, *Tumour necrosis factor (TNFalpha) as a novel therapeutic target in symptomatic corticosteroid dependent asthma,* Thorax, **60** (2005), 1012–1018.
[46] A. Jansson, M. Fagerlind, D. Karlsson, P. Nilsson and M. Cooley, *In silico simulations suggest that Th-cell development is regulated by both selective and instructive mechanisms,* Immunol. Cell Biol., **84** (2006), 218–226.
[47] A. Jansson, M. Harlen, S. Karlsson, P. Nilsson and M. Cooley, *3D computation modelling of the influence of cytokine secretion on Th-cell development suggests that negative selection (inhibition of Th1 cells) is more effective than positive selection by IL-4 for Th2 cell dominance modelling Th cell selection,* Immunology and Cell Biology, **85** (2007), 189–196.
[48] S. Jeon, S. Oh, H. Park, Y. Kim, E. Shim, H. Lee, M. Oh, B. Bang, E. Chun, S. Kim, Y. Gho, Z. Zhu, Y. Kim and Y. Kim, *TH2 and TH1 lung inflammation induced by airway allergen*

sensitization with low and high doses of double-stranded RNA, J. Allergy Clin. Immunol., **120** (2007), 803–812.

[49] T. Katakai, K. Mori, T. Masuda and A. Shimizu, *Differential localization of Th1 and Th2 cells in autoimmune gastritis,* Int. Immunol., **10** (1998), 1325–1334.

[50] Y. Kim and A. Friedman, *Interaction of tumor with its microenvironment : A mathematical model,* Bull. Math. Biol., **72** (2010), 1029–1068.

[51] Y. Kim, S. Lawler, M. Nowicki, E. Chiocca and A. Friedman, *A mathematical model of brain tumor: Pattern formation of glioma cells outside the tumor spheroid core*, J. Theo. Biol., **260** (2009), 359–371.

[52] Y. Kim and S. Lim, *The role of the microenvironment in tumor invasion,* 2009 Proceedings of the Fourth SIAM Conference on Mathematics for Industry (MI09), (2010), 84–92.

[53] Y. Kim, S. Oh, S. Jeon, H. Park, S. Lee, E. Chun, B. Bang, H. Lee, M. Oh, Y. Kim, J. Kim, Y. Gho, S. Cho, K. Min, Y. Kim and Z. Zhu, *Airway exposure levels of lipopolysaccharide determine type 1 versus type 2 experimental asthma,* J. Immunol., **178** (2007), 5375–5382.

[54] Y. Kim, M. Stolarska and H. Othmer, *The role of the microenvironment in tumor growth and invasion,* Progress in Biophysics and Molecular Biology, **106** (2011), 353–379.

[55] Y. Kim, J. C. S.W. Hong, T. Shin, H. Moon and E. C. et al., *Vascular endothelial growth factor is a key mediator in the development of T cell priming and its polarization to type 1 and type 17 T helper cells in the airways,* J. Immunol., **183** (2009), 5113–5120.

[56] Y. Kim, J. Wallace, F. Li, M. Ostrowski and A. Friedman, *Transformed epithelial cells and fibroblasts/myofibroblasts interaction in breast tumor: a mathematical model and experiments,* J. Math. Biol., **61** (2010), 401–421.

[57] J. Kirberg, A. Berns and H. Boehmer, *Peripheral T cell survival requires continual ligation of the T cell receptor to major histocompatibility complex-encoded molecules,* J. Exp. Med., **186** (1997), 1269–1275.

[58] D. Kirschner and J. Panetta, *Modeling immunotherapy of the tumor-immune interaction,* J. Math. Biol., **37** (1998), 235–252.

[59] L. Kreuz and A. Levy, *Physical properties of chick interferon*, J. Bacteriology, **89** (1965), 462–469.

[60] H. Kuipers, D. Hijdra, V. Vries, H. Hammad, J. Prins, A. Coyle, H. Hoogsteden and B. Lambrecht, *Lipopolysaccharide-induced suppression of airway Th2 responses does not require IL-12 production by dendritic cells,* J. Immunol., **171** (2003), 3645–3654.

[61] R. Kumar, D. Webb, C. Herbert and P. Foster, *Interferon-gamma as a possible target in chronic asthma,* Inflamm. Allergy Drug Targets, **5** (2006), 253–256.

[62] C. Langrish, Y. Chen., W. M. Blumenschein, J. Mattson, B. Basham, J. Sedgwick, T. McClanahan, R. Kastelein and D. Cua, *Il-23 drives a pathogenic T cell population that induces autoimmune inflammation,* J. Exp. Med., **201** (2005), 233–240.

[63] Y. Lee, H. Turner, C. Maynard, J. Oliver, D. Chen, C. Elson and C. Weaver, *Late developmental plasticity in the T helper 17 lineage,* Immunity, **30** (2009), 92–107.

[64] C. M. Lloyd and C. M. Hawrylowicz, *Regulatory T cells in asthma,* Immunity, **31** (2009), 438–449.

[65] H. Lortat-Jacob, F. Baltzer and J. Grimaud, *Heparin decreases the blood clearance of interferon-gamma and increases its activity by limiting the processing of its carboxyl-terminal sequence*, The Journal of Biological Chemistry, **271** (1996), 16139–16143.

[66] G. Lugo-Villarino, R. Maldonado-Lopez, R. Possemato, C. Penaranda and L. Glimcher, *T-bet is required for optimal production of IFN-gamma and antigen-specific t cell activation by dendritic cells,* Proc. Natl. Acad. Sci. USA, **100** (2003), 7749–7754.

[67] A. Magnan, L. Mély, C. Camilla, M. Badier, F. Montero-Julian, C. Guillot, B. Casano, S. Prato, V. Fert, P. Bongrand and D. Vervloet, *Assessment of the Th1/Th2 paradigm in whole blood in atopy and asthma. Increased IFN-gamma-producing CD8(+) T cells in asthma,* Am. J. Respir. Crit. Care Med., **161** (2000), 1790–1796.

[68] S. Marino, I. Hogue, C. Ray and D. Kirschner, *A methodology for performing global uncertainty and sensitivity analysis in systems biology,* J. Theor. Biol., **254** (2008), 178–196.

[69] M. Masoli, D. Fabian, S. Holt and R. Beasley, *The global burden of asthma: Executive summary of the GINA dissemination committee report,* Allergy, **59** (2004), 469–478.

[70] G. Mazzarella, A. Bianco, E. Catena, R. De Palma and G. Abbate, *Th1/Th2 lymphocyte polarization in asthma,* Allergy, **55** (2000), 6–9.

[71] O. Michel, R. Ginanni, J. Duchateau, F. Vertongen, B. Bon and R. Sergysels, *Domestic endotoxin exposure and clinical severity of asthma,* Clin. Exp. Allergy, **21** (1991), 441–448.

[72] M. Miller, S. Wei, I. Parker and M. Cahalan, *Two-photon imaging of lymphocyte motility and antigen response in intact lymph node,* Science, **296** (2002), 1869–1873.
[73] H.-G. Moon, Y.-M. Tae, Y.-S. Kim, S. Gyu Jeon, S.-Y. Oh, Y. Song Gho, Z. Zhu and Y.-K. Kim, *Conversion of Th17-type into Th2-type inflammation by acetyl salicylic acid via the adenosine and uric acid pathway in the lung,* Allergy, **65** (2010), 1093–1103.
[74] B. Morel, J. Kalagnanam and P. Morel, *Mathematical modelling of Th1-Th2 dynamics,* in "Theoretical and Experimental Insights into Immunology" (eds. A. S. Perelson and G. Weisbuch), chapter H66 Nato ASI, Springer-Verlag, Berlin, Germany, (1992), 171–189.
[75] J. Morjaria, K. Babu, S. Holgate and R. Polosa, *Tumour necrosis factor-alpha as a therapeutic target in asthma,* Drug Discovery Today: Therapeutic Strategies, **3** (2006), 309–316.
[76] J. Morjaria, K. Babu, R. Polosa and S. Holgate, *Tumour necrosis factor-alpha in severe corticosteroid-refractory asthma,* Exp. Rev. Resp. Med., **1** (2007), 51–63.
[77] T. Mosmann, H. Cherwinski, M. Bond, M. Giedlin and R. Coffman, *Two types of murine helper T cell clone. I. Definition according to profiles of lymphokine activities and secreted proteins,* J. Immunol., **136** (1986), 2348–2357.
[78] T. Mosmann and R. Coffman, *TH1 and TH2 cells: Different patterns of lymphokine secretion lead to different functional properties,* Annu. Rev. Immunol., **7** (1989), 145–173.
[79] E. Muraille, O. Leo and M. Kaufman, *The role of antigen presentation in the regulation of class-specific (Th1/Th2) immune responses,* J. Biol. Syst., **3** (1995), 397–408.
[80] A. Murphy, "Asthma in Focus," In Focus Series, Pharmaceutical Press, 2007.
[81] K. Murphy, P. Travers and M. Walport, "Janeway's Immunobiology," 7^{th} edition, Garland Science Publishing, New York, 2007.
[82] L. Narhi, J. Philo, T. Li, M. Zhang, B. Samal and T. Arakawa, *Induction of alpha-helix in the beta-sheet protein tumor necrosis factor-alpha: Acid-induced denaturation,* Biochemistry, **35** (1996), 11454–11460.
[83] D. Nesic and S. Vukmanovic, *MHC class I is required for peripheral accumulation of CD8+ thymic emigrants,* J. Immunol., **160** (1998), 3705–3712.
[84] S. Olenchock, J. May, D. Pratt and P. Morey, *Occupational exposures to airborne endotoxins in agriculture,* Prog. Clin. Biol. Res., **231** (1987), 475–487.
[85] J. Oliver, L. Bland, C. Oettinger, M. Arduino, S. McAllister, S. Aguero and M. Favero, *Cytokine kinetics in an in vitro whole blood model following an endotoxin challenge,* Lymphokine Cytokine Res., **12** (1993), 115–120.
[86] G. J. Pettet, H. M. Byrne, D. L. S. Mcelwain and J. Norbury, *A model of wound-healing angiogenesis in soft tissue,* Math. Bios., **136** (1996), 35–63.
[87] A. Ray, A. Khare, N. Krishnamoorthy, Z. Qi and P. Ray, *Regulatory T cells in many flavors control asthma,* Mucosal. Immunol., **3** (2010), 216–229.
[88] J. Richter, G. Metzner and U. Behn, *Mathematical modelling of venom immunotherapy,* Journal of Theoretical Medicine, **4** (2002), 119–132.
[89] D. S. Robinson, *Regulatory T cells and asthma,* Clin. Exp. Allergy., **39** (2009), 1314–1323.
[90] R. Rooke, C. Waltzinger, C. Benoist and D. Mathis, *Targeted complementation of MHC class II deficiency by intrathymic delivery of recombinant adenoviruses,* Immunity, **7** (1997), 123–134.
[91] C. Ruedl, M. Bachmann and M. Kopf, *The antigen dose determines t helper subset development by regulation of CD40 ligand,* Eur. J. Immunol., **30** (2000), 2056–2064.
[92] S. Sakaguchi, *Regulatory T cells: Key controllers of immunologic self-tolerance,* Cell, **101** (2000), 455–458.
[93] J. Scheel, S. Weimans, A. Thiemann, E. Heisler and M. Hermann, *Exposure of the murine RAW 264.7 macrophage cell line to hydroxyapatite dispersions of various composition and morphology: Assessment of cytotoxicity, activation and stress response,* Toxicol. in Vitro, **23** (2009), 531–538.
[94] A. Schwingshackl, M. Duszyk, N. Brown and R. Moqbel, *Human eosinophils release matrix metalloproteinase-9 on stimulation with TNF-alpha,* J. Allergy Clin. Immunol., **104** (1999), 983–990.
[95] D. Stickle, D. Lauffenburger and R. Daniele, *The motile response of lung macrophages: Theoretical and experimental approaches using the linear under-agarose assay,* J. Leukoc. Biol., **38** (1985), 383–401.
[96] C. L. Stokes and D. A. Lauffenburger, *Analysis of the roles of microvessel endothelial cell random motility and chemotaxis in angiogenesis,* J. Theor. Biol., **152** (1991), 377–403.

[97] E. Suzuki, A. Tsutsumi, D. Goto, I. Matsumoto, S. Ito, M. Otsu, M. Onodera, S. Takahashi, Y. Sato and T. Sumida, *Gene transduction of tristetraprolin or its active domain reduces TNF-alpha production by Jurkat T cells,* Int. J. Mol. Med., **17** (2006), 801–809.

[98] M. Swanson, W. Lee and V. Sanders, *IFN-gamma production by Th1 cells generated from naive CD4+ T cells exposed to norepinephrine,* J. Immunol., **166** (2001), 232–240.

[99] S. Takeda, H. Rodewald, H. Arakawa, H. Bluethmann and T. Shimizu, *MHC class II molecules are not required for survival of newly generated CD4+ T cells, but affect their long-term life span,* Immunity, **5** (1996), 217–228.

[100] R. Tyson, L. Stern and R. LeVeque, *Fractional step methods applied to a chemotaxis model,* J. Math. Biol., **41** (2000), 455–475.

[101] R. Vogel and U. Behn, *Th1-Th2 regulation and allergy: Bifurcation analysis of the non-autonomous system*, in "Mathematical Modeling of Biological Systems," Volume II (eds. A. Deutsch, R. Parra, R. J. de Boer, O. Diekmann, P. Jagers, E. Kisdi, M. Kretzschmar, P. Lansky, and H. Metz), Modeling and Simulation in Science, Engineering and Technology, Birkhäuser Boston, (2008), 145–155.

[102] Y. Wan, *Multi-tasking of helper T cells,* Immunology, **130** (2010), 166–171.

[103] Y. Wang, K. Voo, B. Liu, C. Chen, B. Uygungil and W. Spoede, J. Bernstein, D. Huston and Y. Liu, *A novel subset of CD4(+) T(H)2 memory/effector cells that produce inflammatory IL-17 cytokine and promote the exacerbation of chronic allergic asthma,* J. Exp. Med., **207** (2010), 2479–2491.

[104] M. Wills-Karp, J. Luyimbazi, X. Xu, B. Schofield, T. Neben, C. Karp and D. Donaldson, *Interleukin-13: Central mediator of allergic asthma,* Science, **282** (1998), 2258–2261.

[105] M. Wills-Karp, J. Santeliz and C. L. Karp, *The germless theory of allergic disease: Revisiting the hygiene hypothesis,* Nat. Rev. Immunol., **1** (2001), 69–75.

[106] D. Witherden, N. van Oers, C. Waltzinger, A. Weiss, C. Benoist and D. Mathis, *Tetracycline-controllable selection of CD4(+) T cells: Half-life and survival signals in the absence of major histocompatibility complex class II molecules,* J. Exp. Med., **191** (2000), 355–364.

[107] M. Yang, R. Kumar and P. Foster, *Interferon-gamma and pulmonary macrophages contribute to the mechanisms underlying prolonged airway hyperresponsiveness,* Clin. Exp. Allergy, **40** (2010), 163–173.

[108] Y. Yang, H.-L. Zhang and J. Wu, *Role of T regulatory cells in the pathogenesis of asthma,* Chest., **138** (2010), 1282–1283.

[109] A. Yates, C. Bergmann, J. V. Hemmen, J. Stark and R. Callard, *Cytokine-modulated regulation of helper T cell populations,* J. Theor. Biol., **206** (2000), 539–560.

[110] A. Yates, R. Callard and J. Stark, *Combining cytokine signalling with T-bet and GATA-3 regulation in Th1 and Th2 differentiation: A model for cellular decision-making,* J. Theor. Biol., **231** (2004), 181–196.

[111] M. Yazdanbakhsh, P. G. Kremsner and R. van Ree, *Allergy, parasites, and the hygiene hypothesis,* Science, **296** (2002), 490–494.

[112] Y. Zhao, J. Yang, Y. Gao and W. Guo, *Th17 immunity in patients with allergic asthma,* Int. Arch. Allergy Immunol., **151** (2010), 297–307.

[113] L. Zhou, I. Ivanov, R. Spolski, R. Min, K. Shenderov, T. Egawa, D. Levy, W. Leonard and D. Littman, *IL-6 programs T(H)-17 cell differentiation by promoting sequential engagement of the IL-21 and IL-23 pathways,* Nat. Immunol., **8** (2007), 967–974.

[114] J. Zhuang and G. Wogan, *Growth and viability of macrophages continuously stimulated to produce nitric oxide,* Proc. Natl. Acad. Sci. USA, **94** (1997), 11875–11880.

Received November 03, 2012; Accepted March 11, 2013.

E-mail address: ahyouhappy@konkuk.ac.kr or ahyouhappy@gmail.com
E-mail address: dlimpid@postech.ac.kr
E-mail address: ssdj80@gmail.com
E-mail address: S.Lawler@leeds.ac.uk
E-mail address: ysgho@postech.ac.kr
E-mail address: juinea@postech.ac.kr
E-mail address: hjhwang@postech.ac.kr